Heidelberg Institute for Theoretical Studies

HITS

Neutron-star properties from the gravitational-wave signal of binary mergers

New frontiers in gravitational wave astrophysics

Rome, 20/06/2017

Andreas Bauswein

(Heidelberg Institute for Theoretical Studies)

with J. A. Clark, K. Chatziioannou, N. Stergioulas, H.-T. Janka

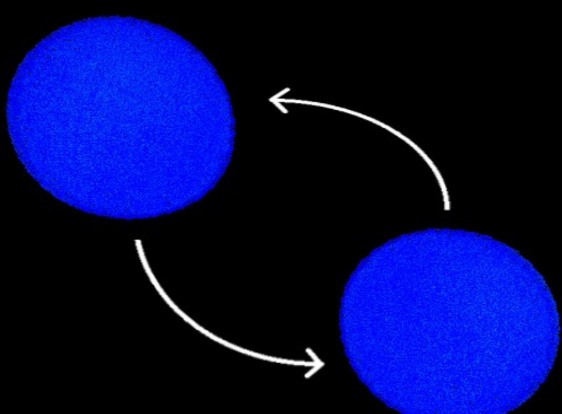

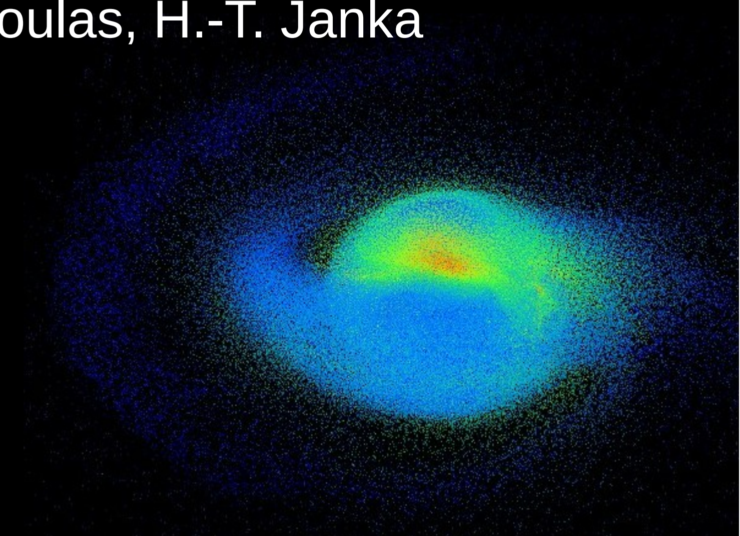

Outline - Motivation

- Threshold for prompt black-hole formation and maximum mass of non-rotating NSs
- Focus on dominant postmerger GW emission → constrain high-density equation of state
- Neutron star radius measurement
- GW data analysis
- Origin of secondary GW features in the postmerger phase
- Classification scheme of postmerger GW spectra based on subdominant peaks

Collapse behavior:

Prompt vs. delayed (/no) collapse

Collapse behavior

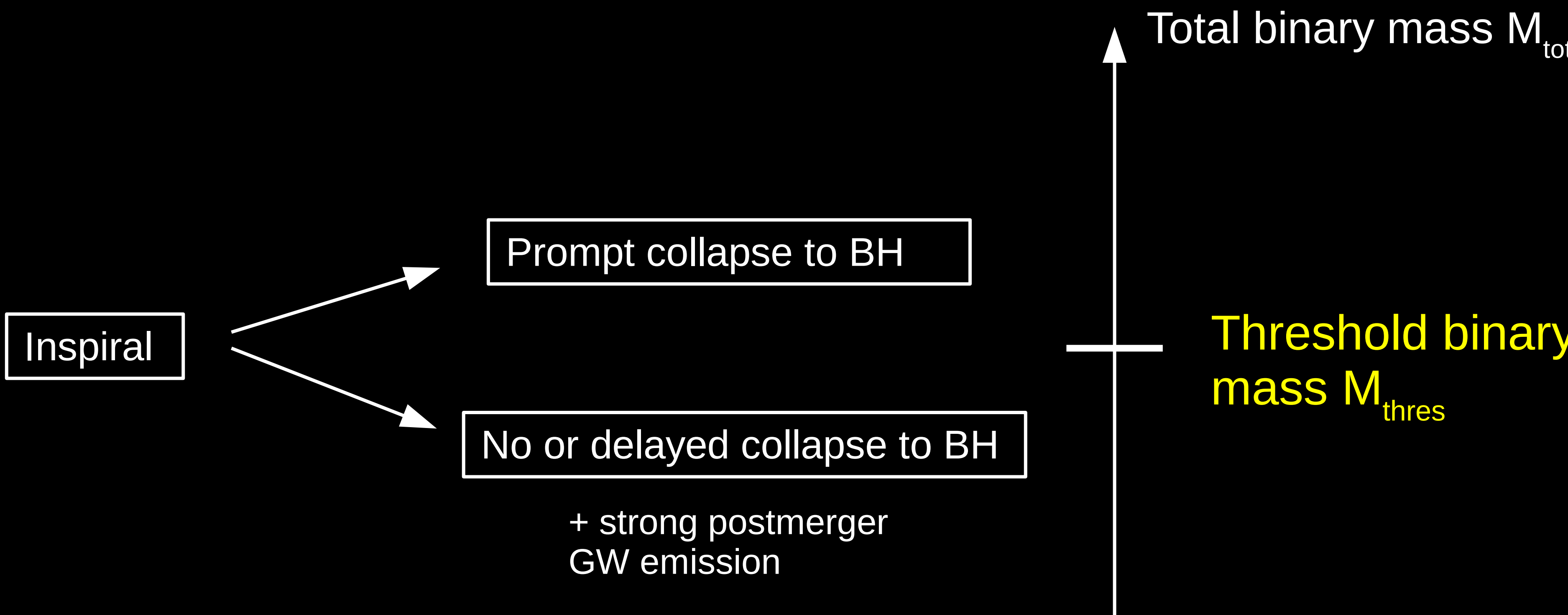

EoS dependent - somehow M_{max} should play a role

→ … from observations we can determine M_{max}, R_{max}, ρ_{max}

Key quantity: Threshold binary mass M_{thres} for prompt BH collapse

Fractional increase of M_{max}

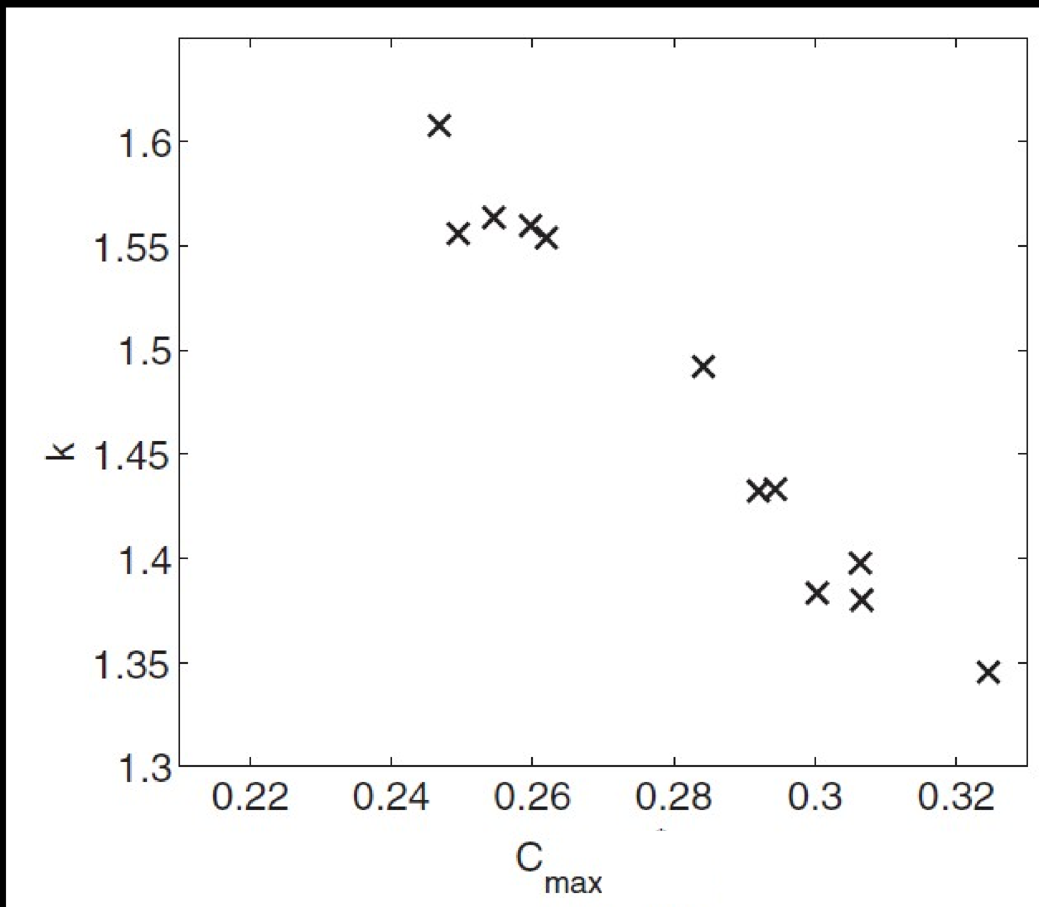

$$M_{thres} = k * M_{max}$$

with $k = k(C_{max})$

$$C_{max} = G\, M_{max} / (c^2\, R_{max})$$

(compactness of TOV maximum-mass configuration)

=> $M_{thres} = M_{thres}(M_{max}, R_{max})$

Bauswein et al. 2013

$$k = \frac{M_{thres}}{M_{max}}$$

← From simulations with different M_{tot}

← TOV property of employed EoS

Constrain M_{max}

- Measure several NS mergers with different M_{tot} – check if postmerger GW emission present

  → M_{thres} estimate

- Radius e.g. from postmerger frequency

$$M_{\rm thres} = \left(-3.38\frac{GM_{\rm max}}{c^2 R_{\rm max}} + 2.43\right) M_{\rm max}$$

- Invert fit

$$M_{\rm thres} = \left(-3.6\frac{G\,M_{\rm max}}{c^2\,R_{1.6}} + 2.38\right)\,M_{\rm max}$$

→ M_{max}

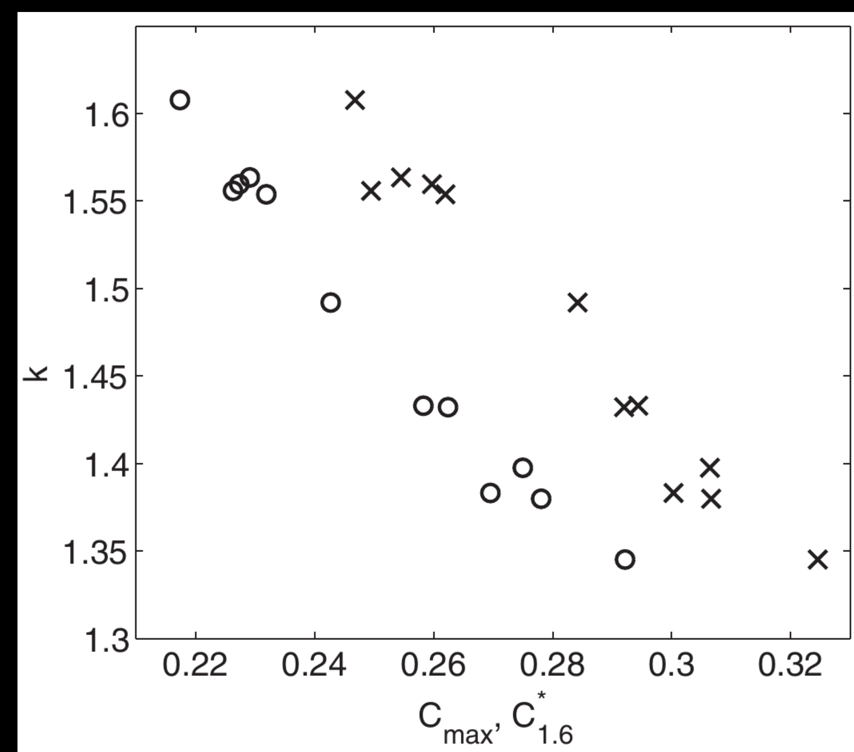

- Note: already a single/few measurement could provide interesting constraints !!!

- M_{thres} constraints also from GRB, em counterparts, …

Semi-analytic model

reproduces / corroborates
collapse behavior

Fractional increase of M_{max}

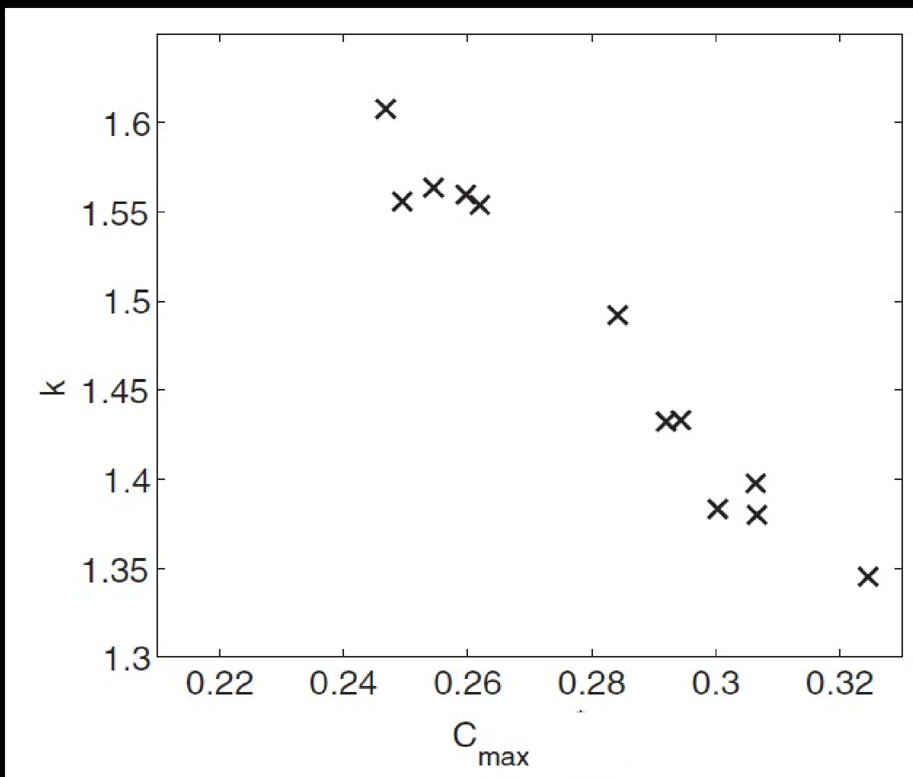

Bauswein et al 2013: numerical determination of collapse threshold through hydrodynamical simulations

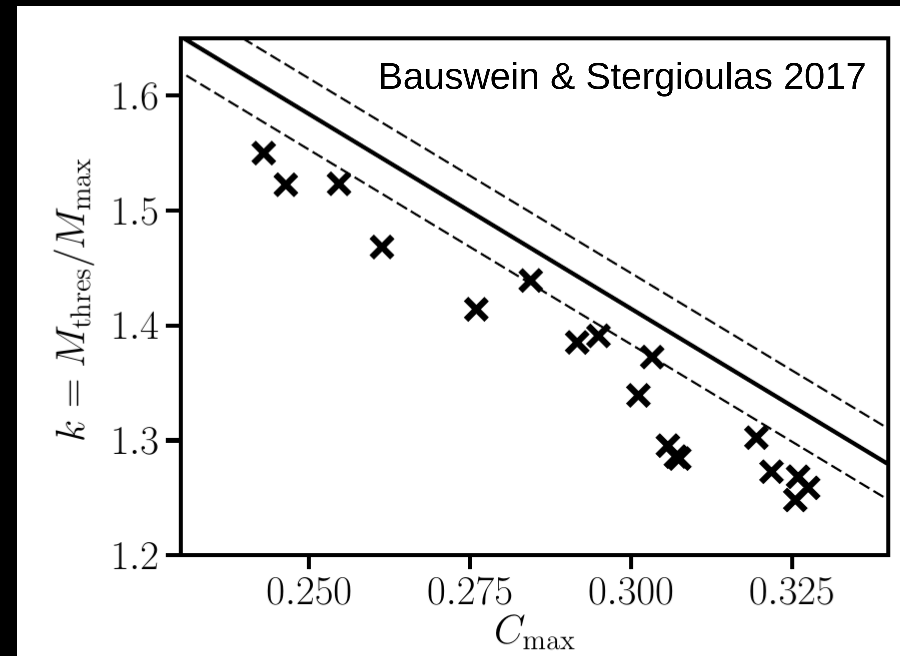

Solid line fit to numerical data

Crosses stellar equilibrium models:

- prescribed (simplistic) diff. rotation
- many EoSs at T=0
- detailed angular momentum budget !

=> equilibrium models qualitatively reproduce collapse behavior

- even quantitatively good considering the adopted approximations

details of the model

- Stellar equilibrium models computed with RNS code (diff. Rotation, T=0, many different microphysical EoS) => turning points => $M_{stab}(J)$
- Compared to $J(M_{tot})$ of merger remnants from simulations (very robust result) → practically independent from simulations

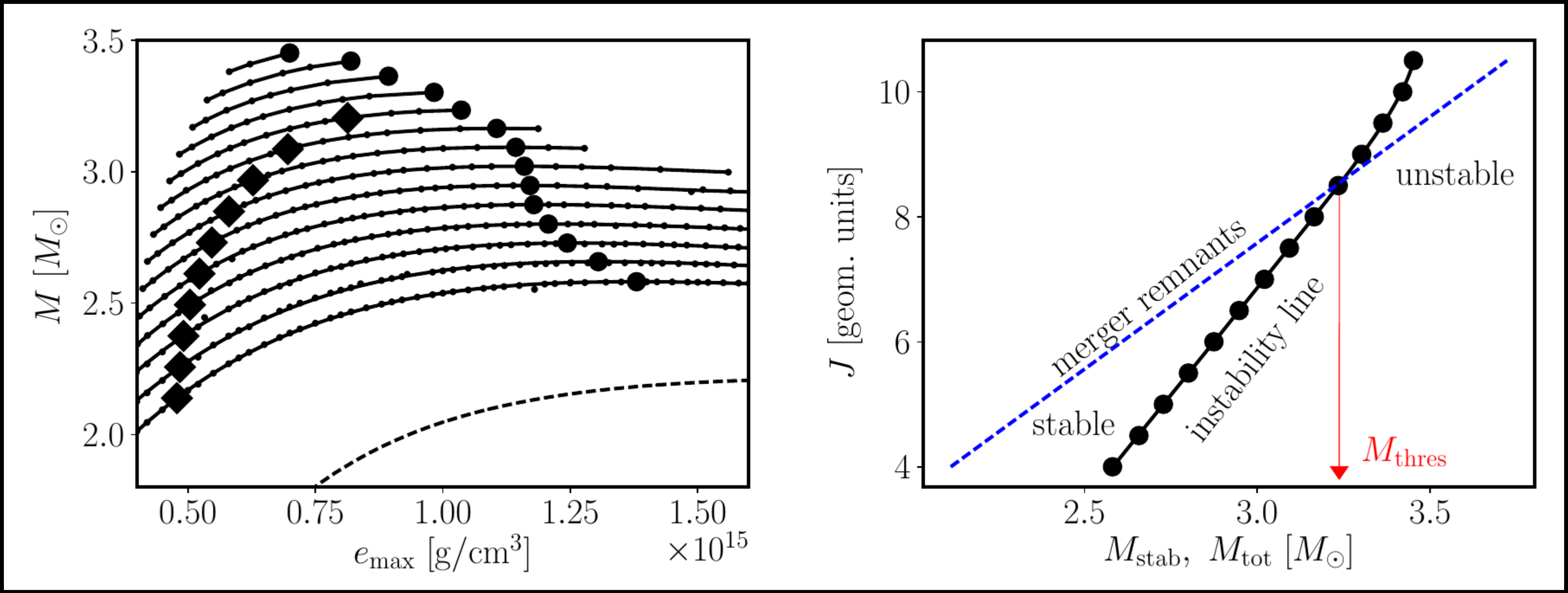

Bauswein & Stergioulas 2017

Radius measurements

Typical GW spectrum

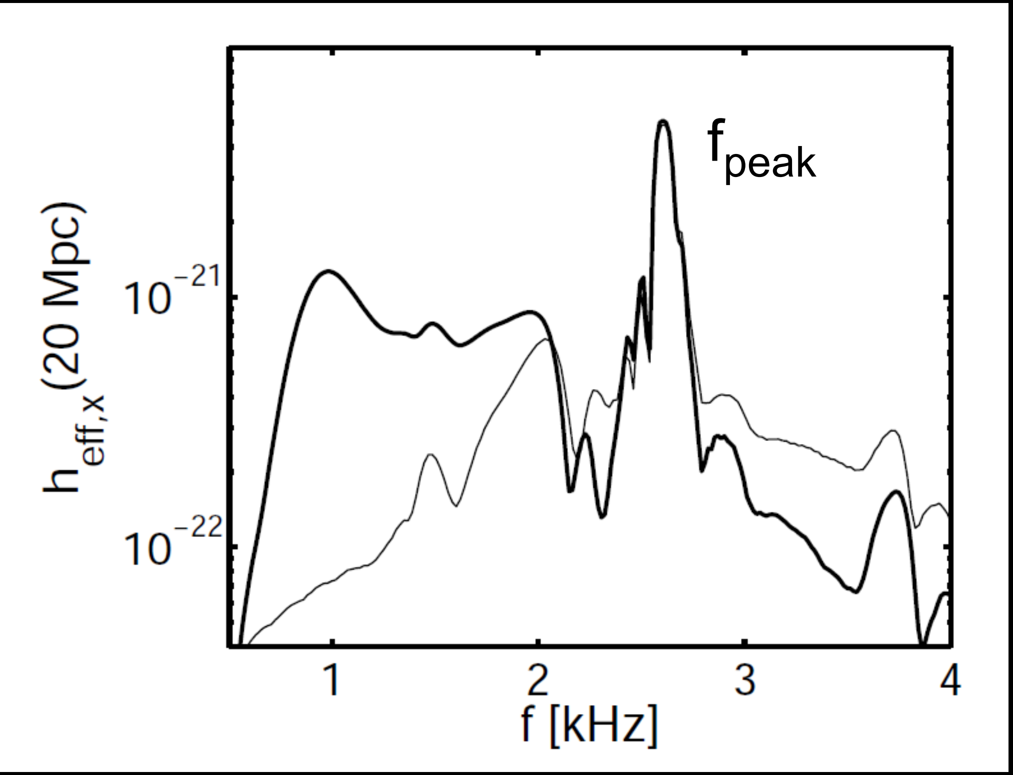

Thin line postmerger only

Note: no unique nomenclature in the literature, e.g. f_{peak} is also called f_2 ...

- Up to 3 pronounced features in postmerger spectrum (f_{peak} + up to two secondary peaks at lower frequencies (subdominant wrt to sensitivity curve; not always present) + structure at higher frequencies)
- f_{peak} robust feature present in all models leading to a NS remnant
- Focus on f_{peak} – in comparison the easiest to measured
- Simulation: 1.35-1.35 M_{sun} DD2 EoS, Smooth Particle Hydro, Conformal Flatness

Gravitational waves – EoS survey

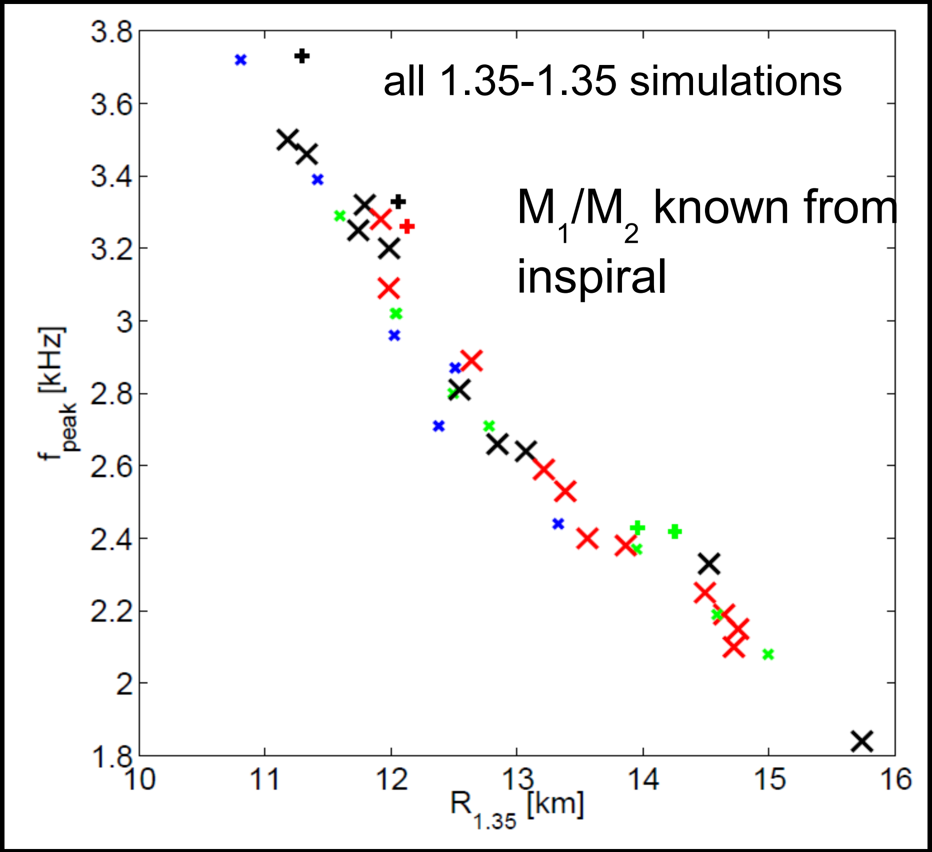

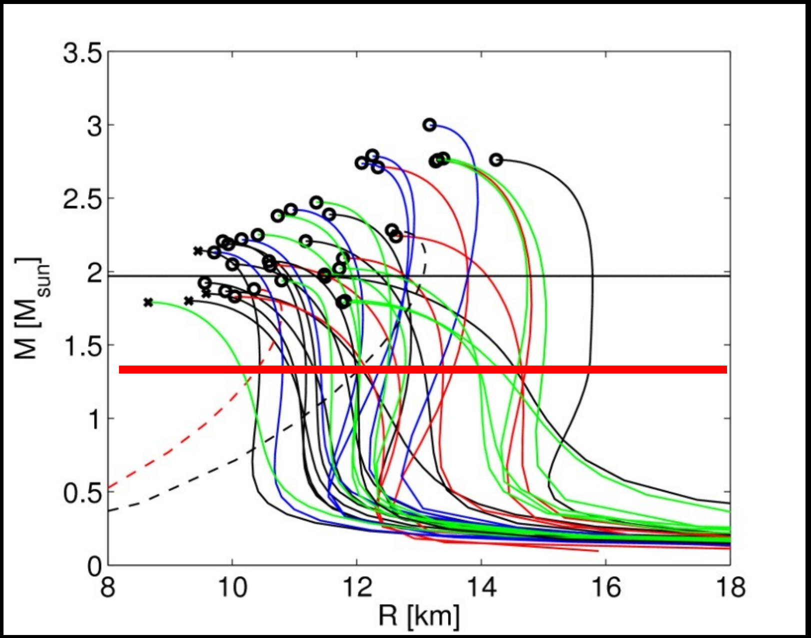

characterize EoS by radius of nonrotating NS with 1.35 M_{sun}

Bauswein et al. 2012

Pure TOV/EoS property => Radius measurement via f_{peak}

Here only 1.35-1.35 Msun mergers (binary masses measurable) – similar relations exist for other fixed binary setups !!!

~ 40 different NS EoSs

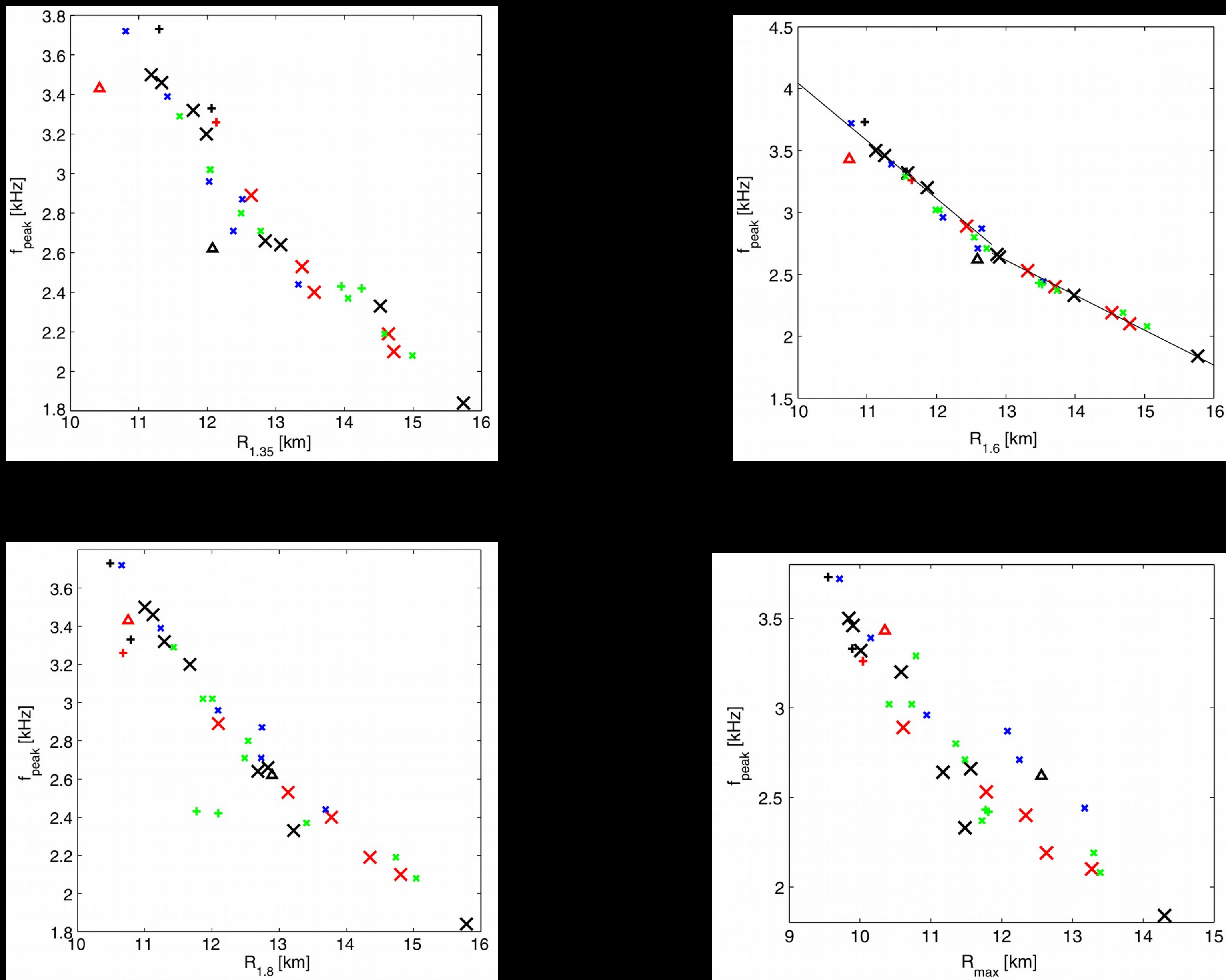

Bauswein et al. 2012

Assess quality of empirical relation relation – only infinity norm meaningful !!!

→ as many EoS models as possible !!!

Gravitational waves – EoS survey

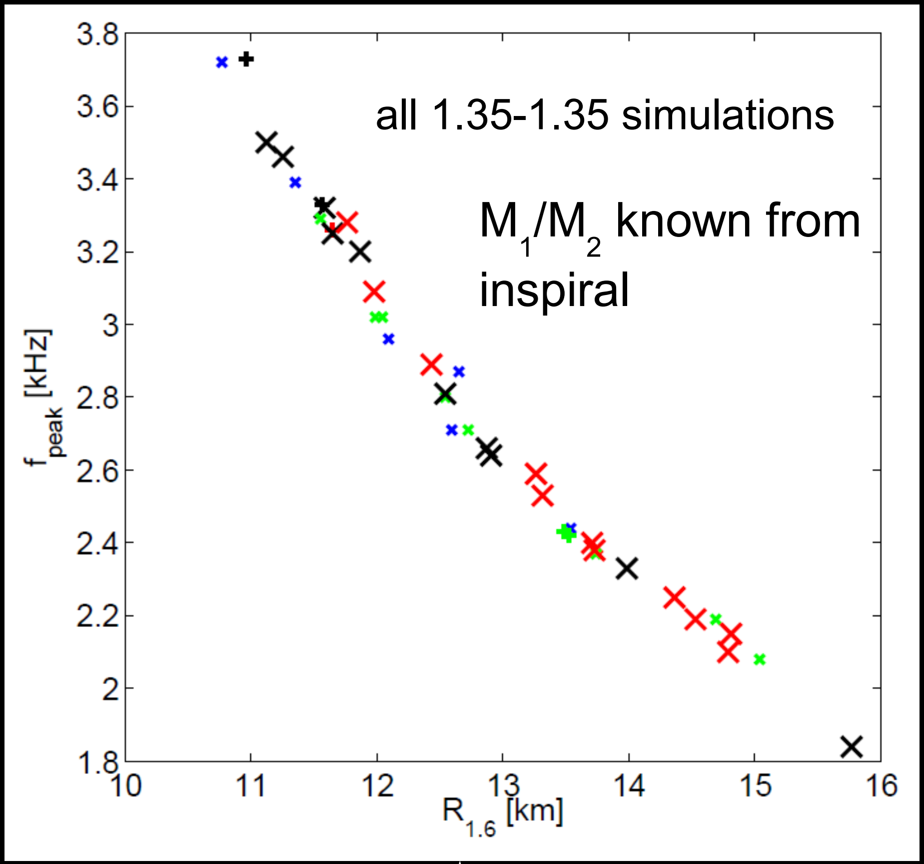

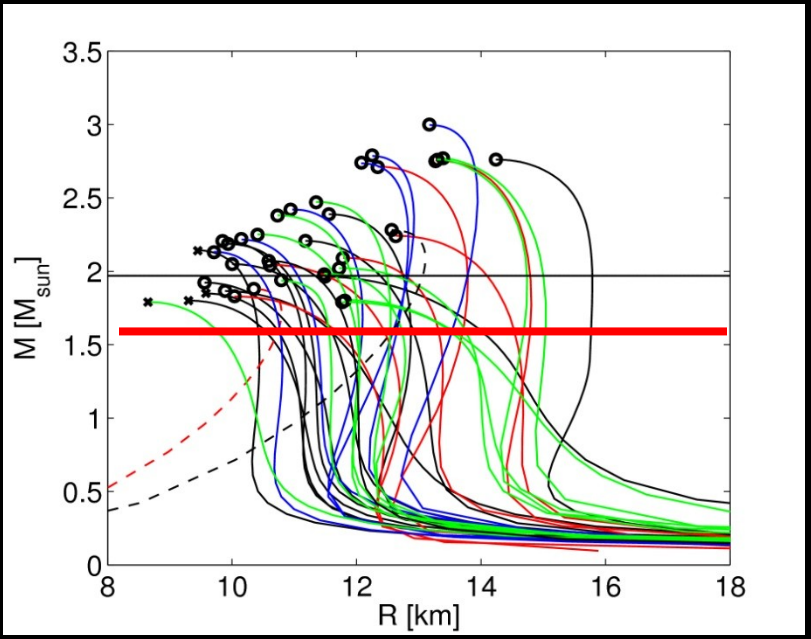

characterize EoS by radius of nonrotating NS with 1.6 M_{sun}

Bauswein et al. 2012

Pure TOV/EoS property => Radius measurement via f_{peak}

Smaller scatter in empirical relation (< 200 m) → smaller error in radius measurement

Note: R of 1.6 M_{sun} NS scales with f_{peak} from 1.35-1.35 M_{sun} mergers (density regimes comparable)

Binary mass variations

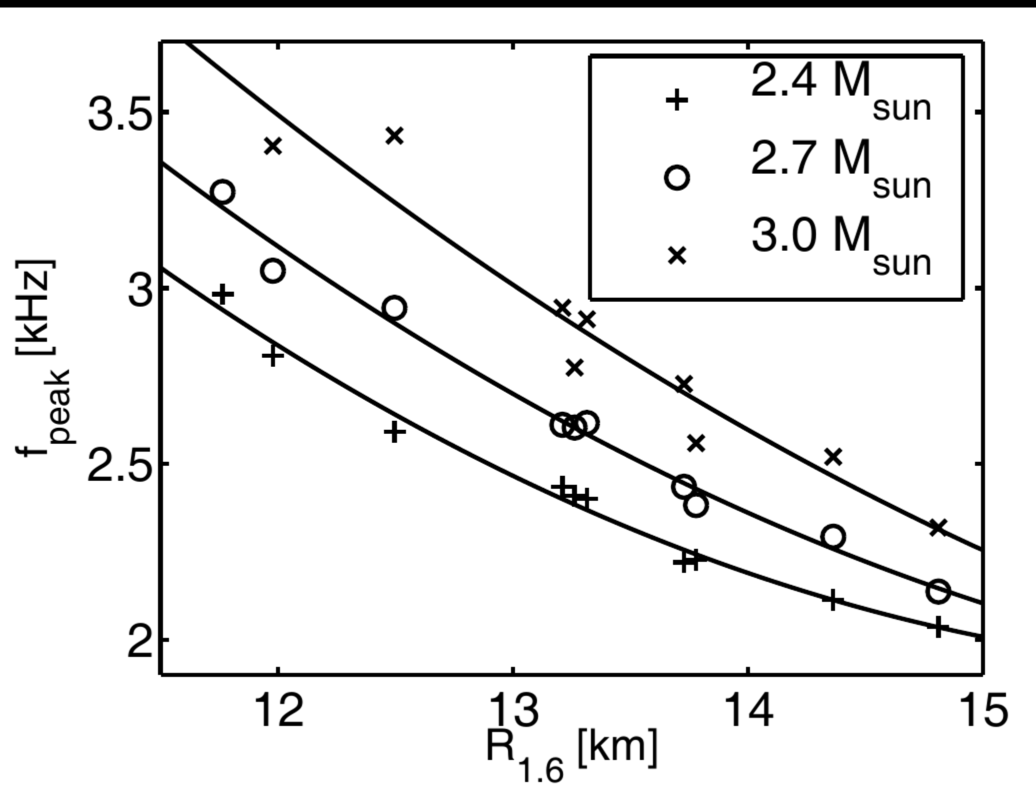

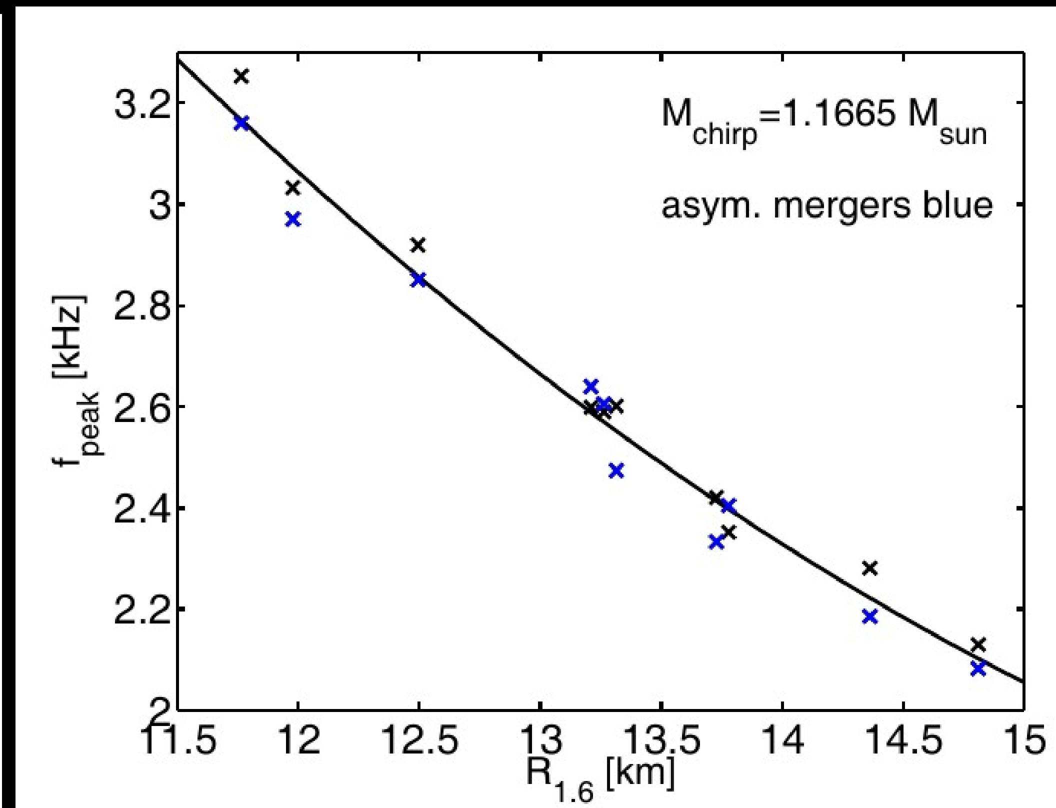

Different total binary masses (symmetric)

Fixed chirp mass (asymmertic 1.2-1.5 M_{sun} binaries and symmetric 1.34-1.34 M_{sun} binaries)

Data analysis: see Clark et al. 2016 (PCA), Clark et al. 2014 (burst search)

→ f_{peak} precisely measurable !!!

Bauswein et al. 2012, 2016

Strategy for radius measurements

- Measure binary masses from inspiral
- Construct f_{peak} – R relation for this fixed binary masses and (optimally) chosen R
- Measure f_{peak} from postmerger GW signal
- Obtain radius by inverting f_{peak} – R relation
- (possibly restrict to fixed mass ratios if mergers with high asymmetry are measured)

- Final error of radius measurement:

  - accuracy of f_{peak} measurement (see Clark et al. 2014, Clark et al. 2016)

  - maximum scatter in f-R relation (important to consider very large sample of EoSs)

  - systematic error in f-R relation

Data analysis

- Principal Component analysis

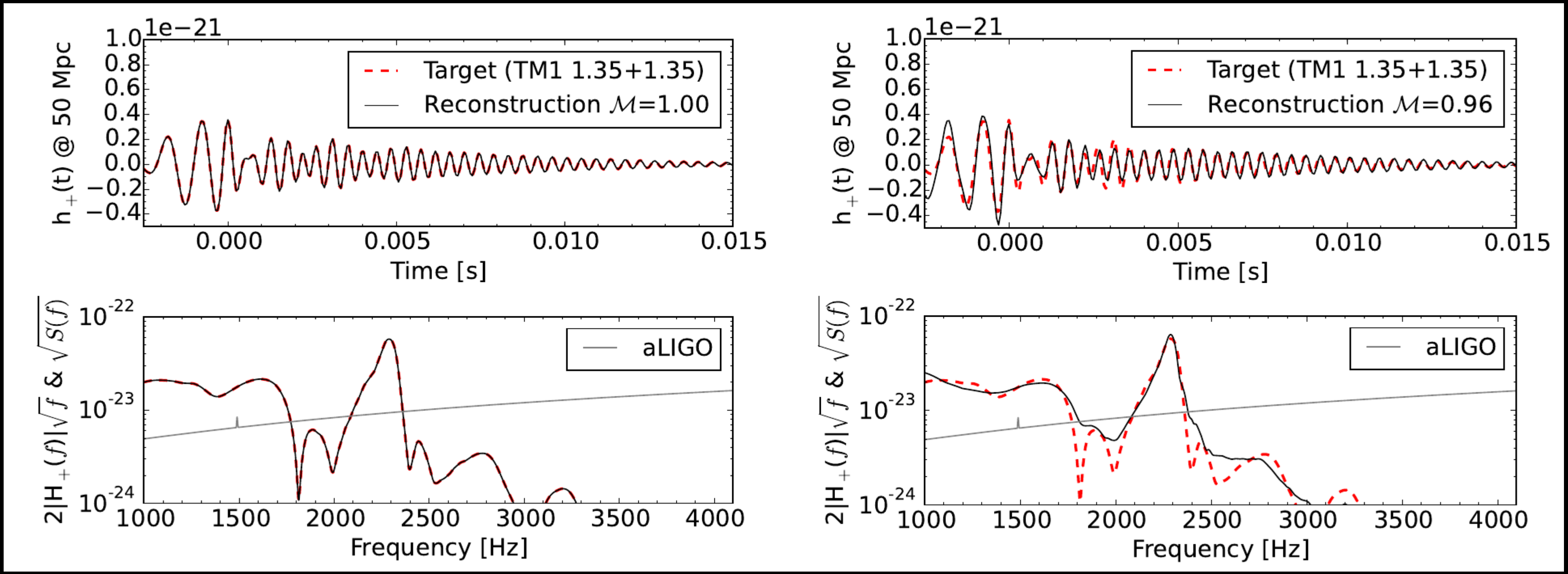

Excluding recovered waveform from catalogue

Clark et al. 2016

studies with unmodeled searches also successful

One more idea for Mmax

(and Rmax, emax, ρmax)

If we get several measurements in the future

Alternative: f_{peak} dependence on total binary mass

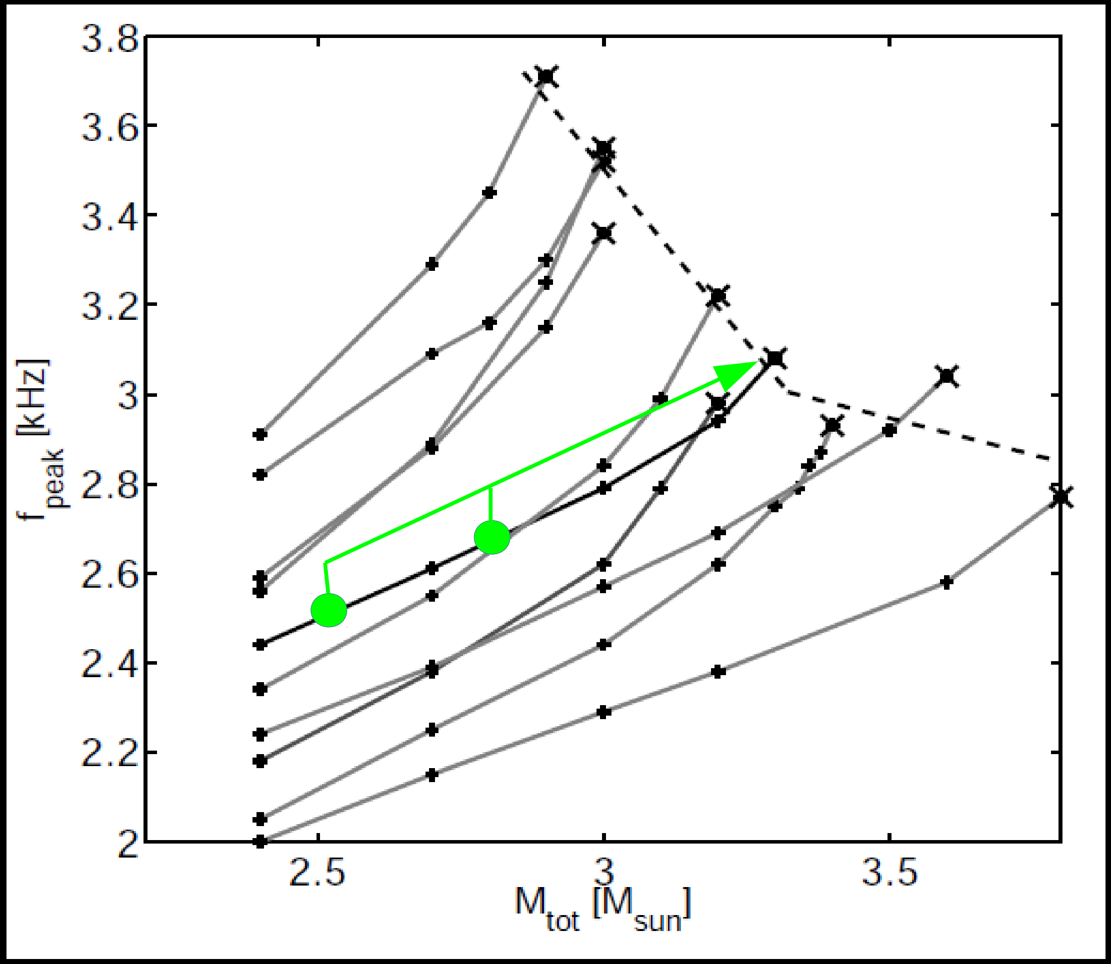

(every single line corresponds to a specific EoS → only one line can be the true EoS)

$$f_{peak} \sim \sqrt{\frac{M}{R^3}}$$

Bauswein et al. 2014

Dominant GW frequency monotone function of M_{tot}

Threshold to prompt BH collapse shows a clear dependence on M_{tot} (dashed line)

from two measurements of f_{peak} at moderate M_{tot}

Maximum-mass TOV properties

by extrapolation of f_{peak} (M_{tot})

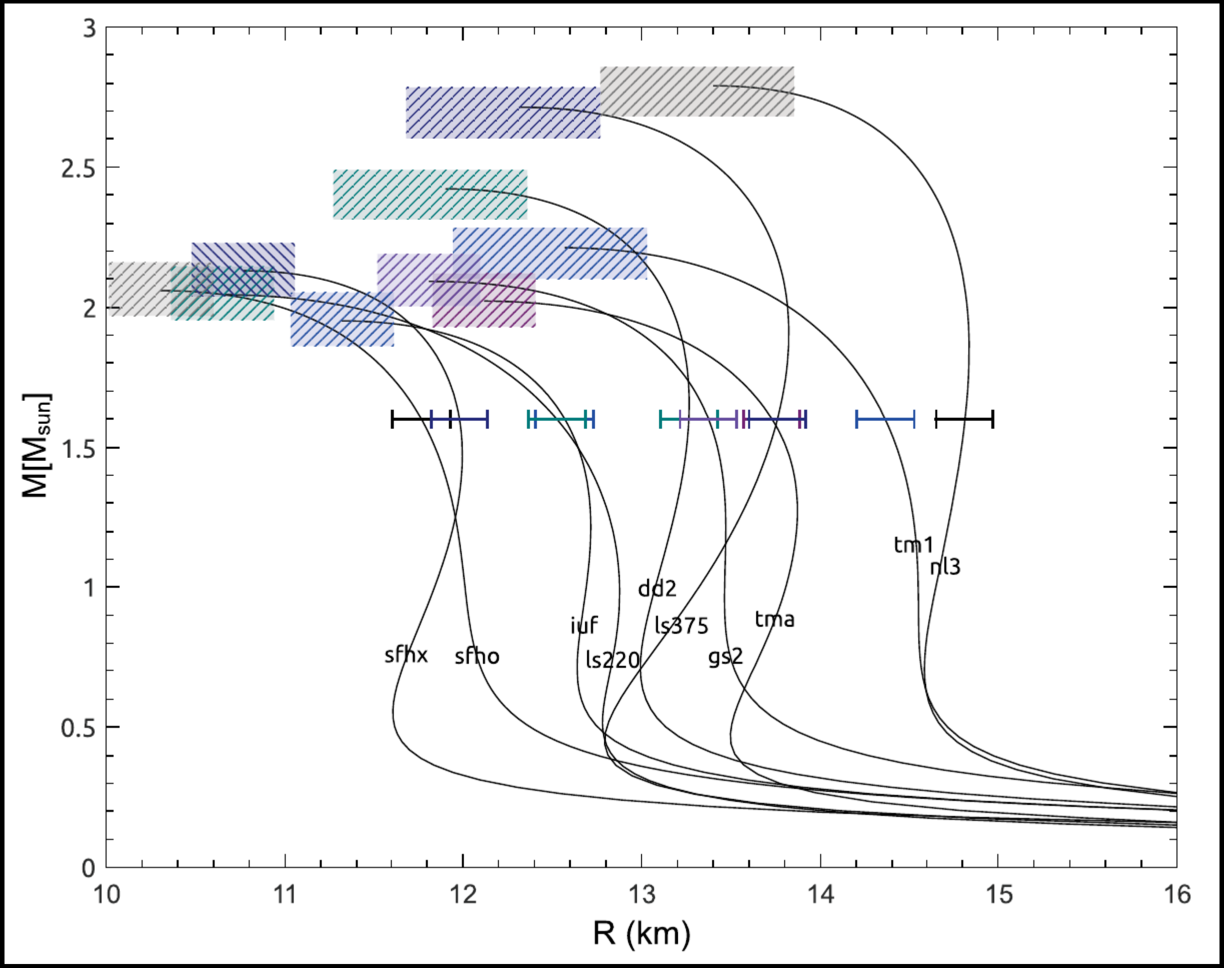

Radius at lower masses from f_{peak}

(final error will depend on EoS and exact systems measured)

Note: M_{thres} may also be constrained from prompt collapse directly

Bauswein et al. 2014

Secondary GW features and postmerger dynamics

Generic GW spectrum

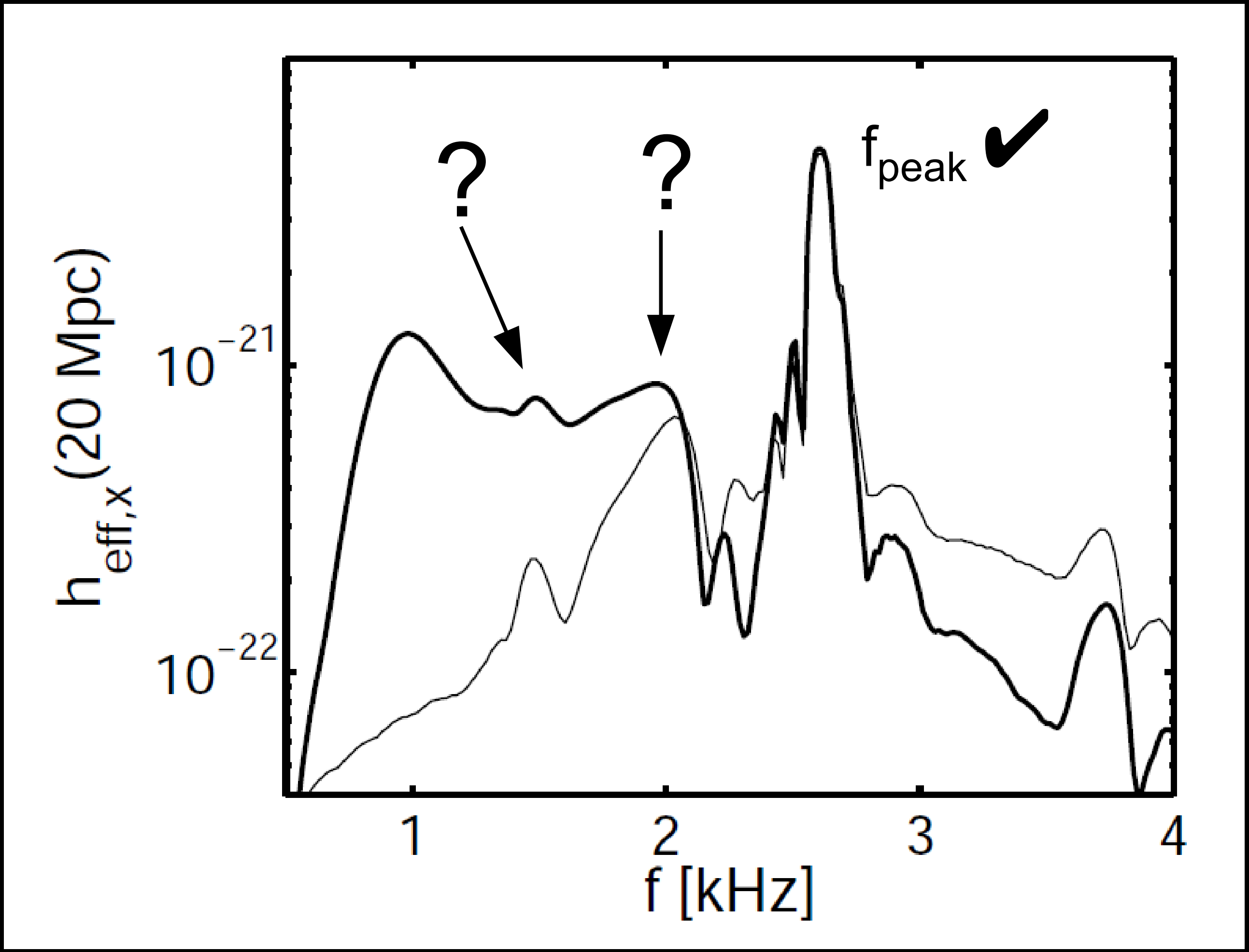

- Up to three pronounced features in the postmerger spectrum (+ structure at higher frequencies)
- 1.35-1.35 Msun DD2 EoS

Interpretation and exact dependencies of secondary frequencies still under debate (cf. Frankfurt group)

Quasi-radial mode

- Central lapse function shows two frequencies (~500 Hz and ~1100 Hz) → clear peaks in FFT
- Add quasi-radial perturbation → re-excite quasi-radial mode => f_0 = 1100 Hz
- Confirmed by mode analysis → radial eigen function at f_0

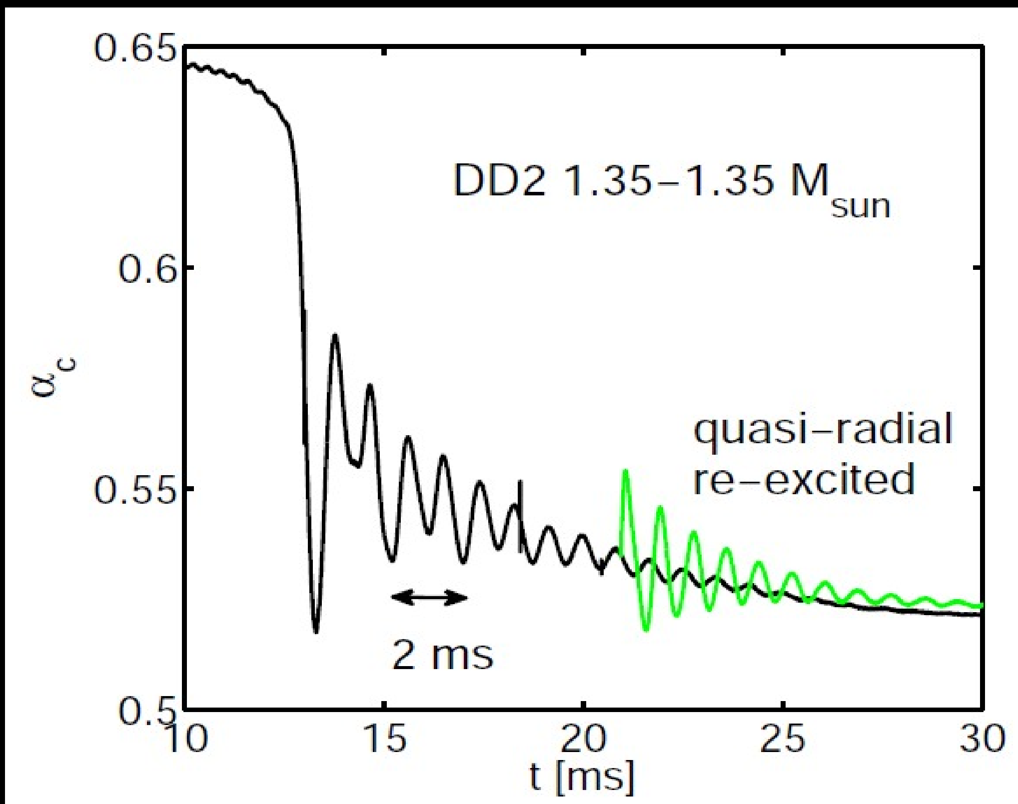

Bauswein et al. 2015

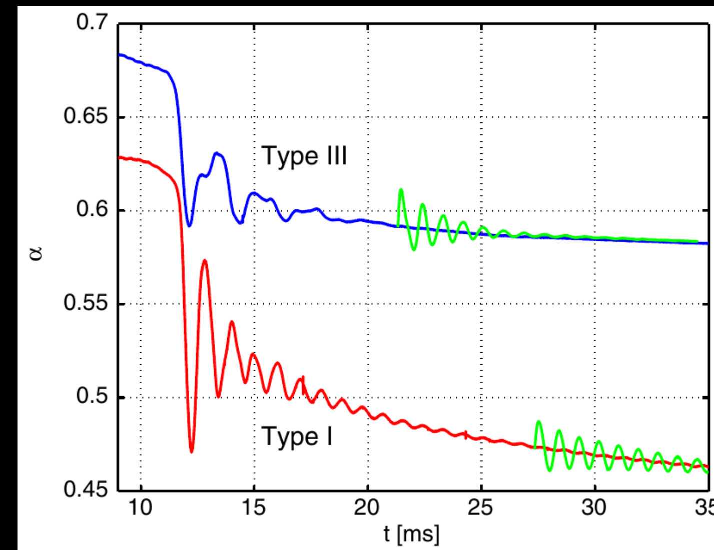

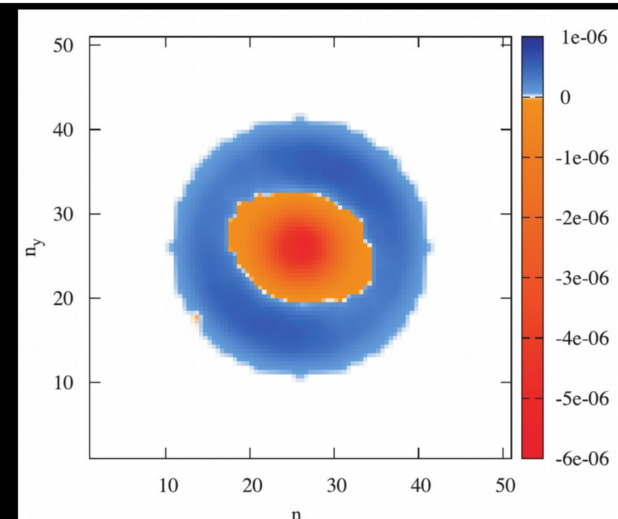

Stergioulas et al. 2011

Could consider also size of the remnant, rhomax, …

Note: additional low-frequency oscillation (500 Hz) also in GW amplitude (explained later)

Generic GW spectrum

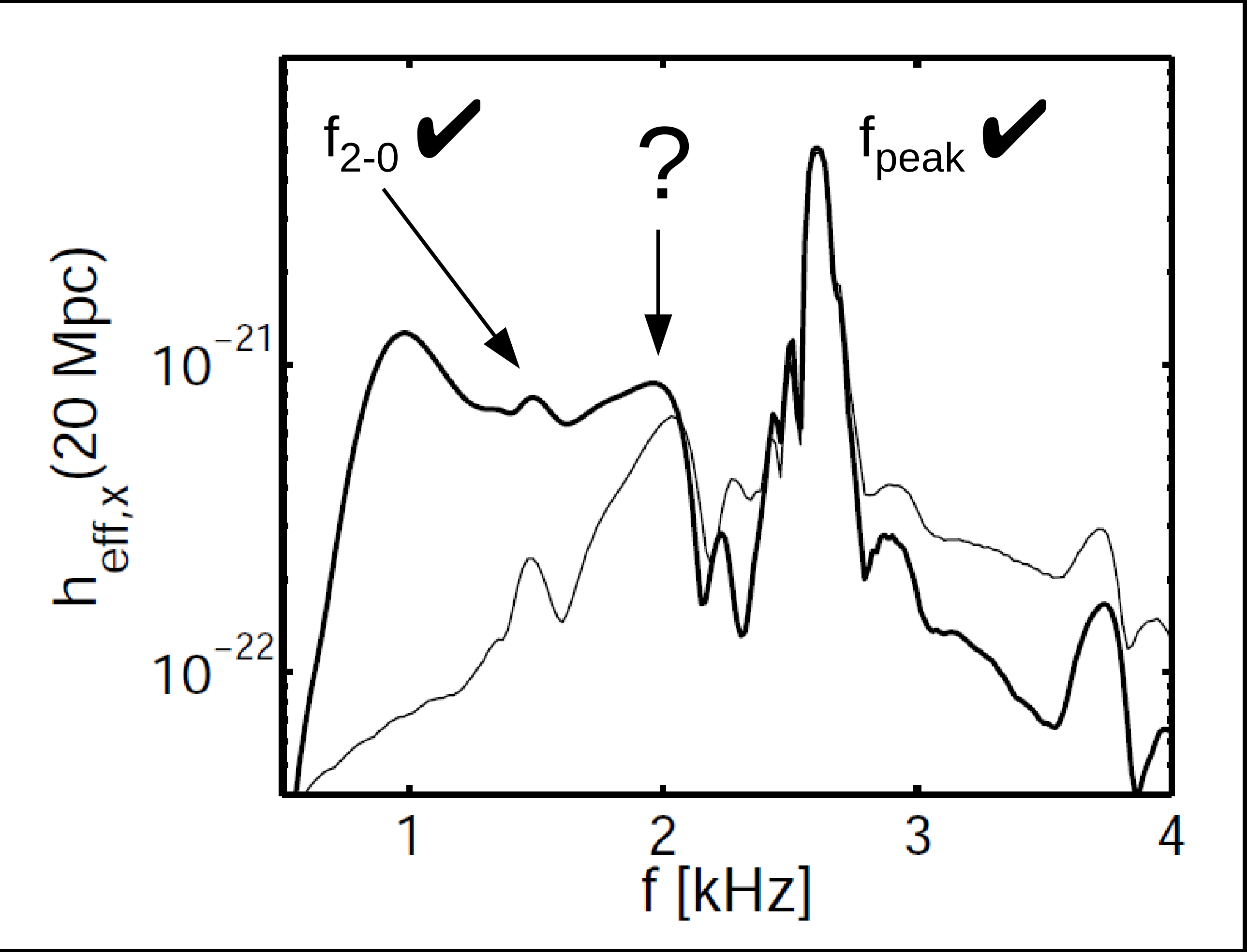

- Interaction between dominant quadrupolar mode and quasi-radial oscillation produced peak at $f_{2\text{-}0} = f_{peak} - f_0$ (see Shibata & Taniguchi 2006, Stergioulas et al. 2011)

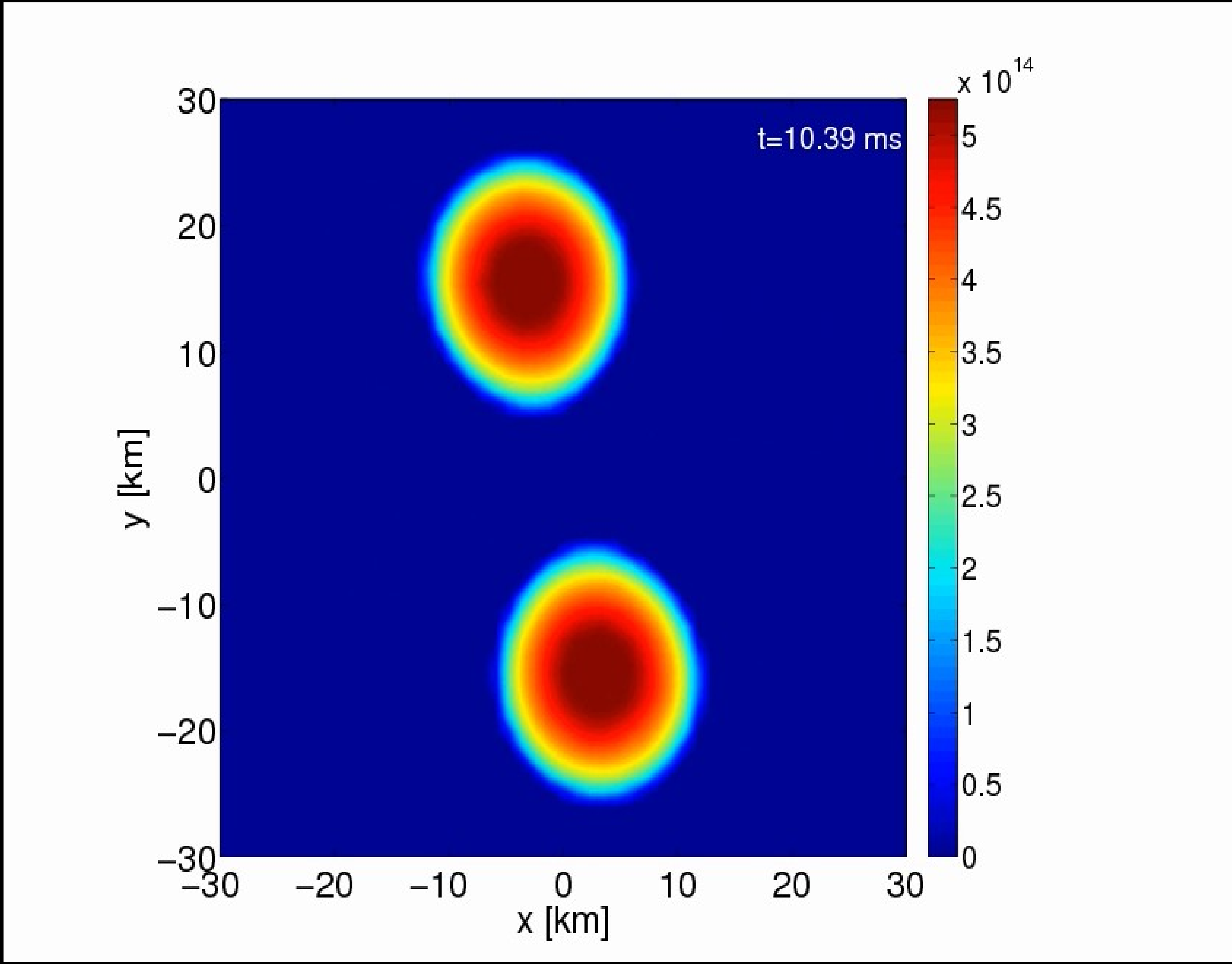
t=10.39 ms
x 10^14
5
4.5
4
3.5
3
2.5
2
1.5
1
0.5
0
30
20
10
0
−10
−20
−30
y [km]
−30
−20
−10
0
10
20
30
x [km]

Antipodal bulges (spiral pattern)

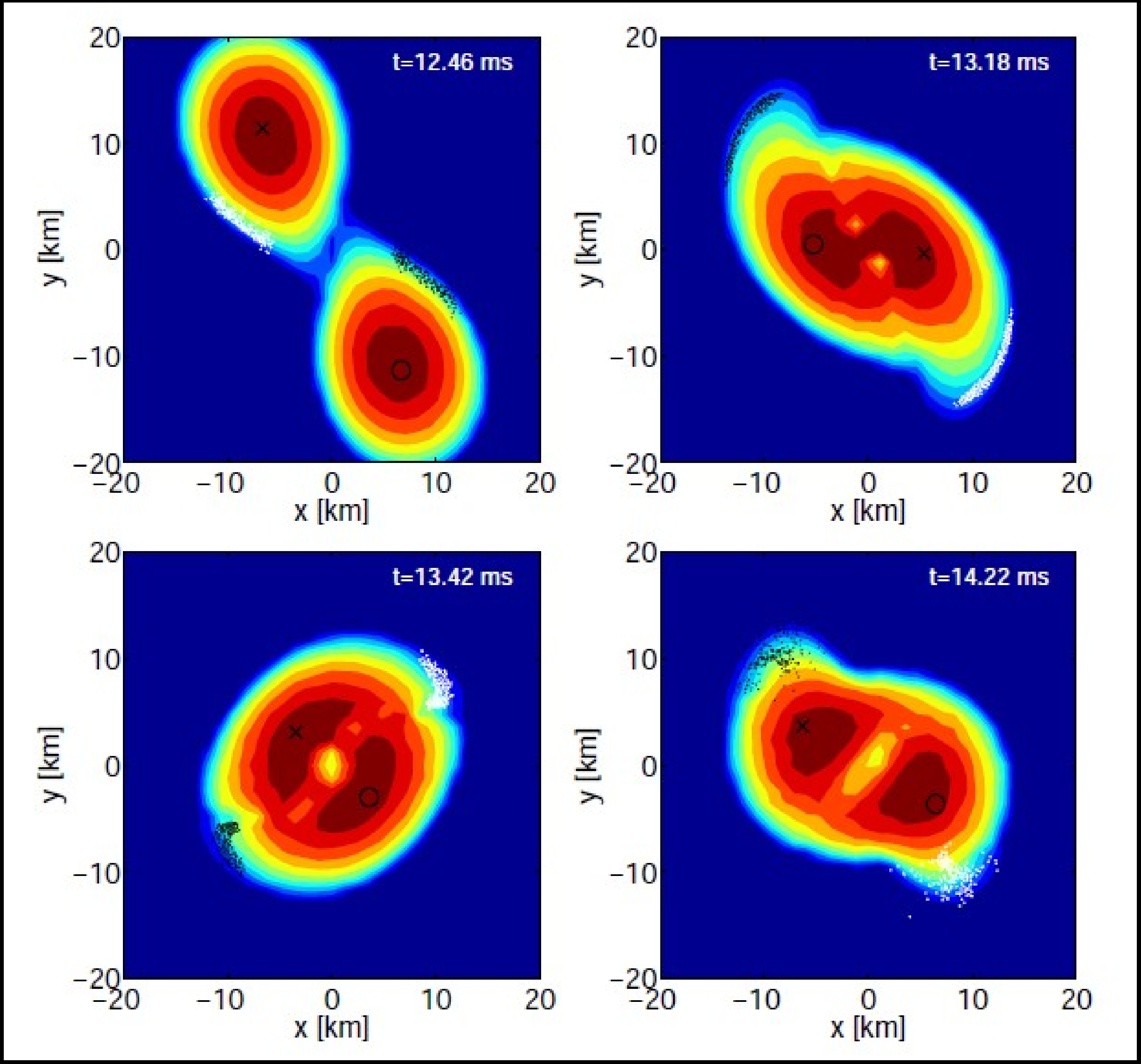

Bauswein et al. 2015

Orbital motion of antipodal bulges slower than inner part of the remnant (double-core structure)

Spiral pattern, created during merging lacks behind

Orbital frequency: 1/1ms → generates GW at 2 kHz !!!

Present for only a few ms / cycles

Generic GW spectrum

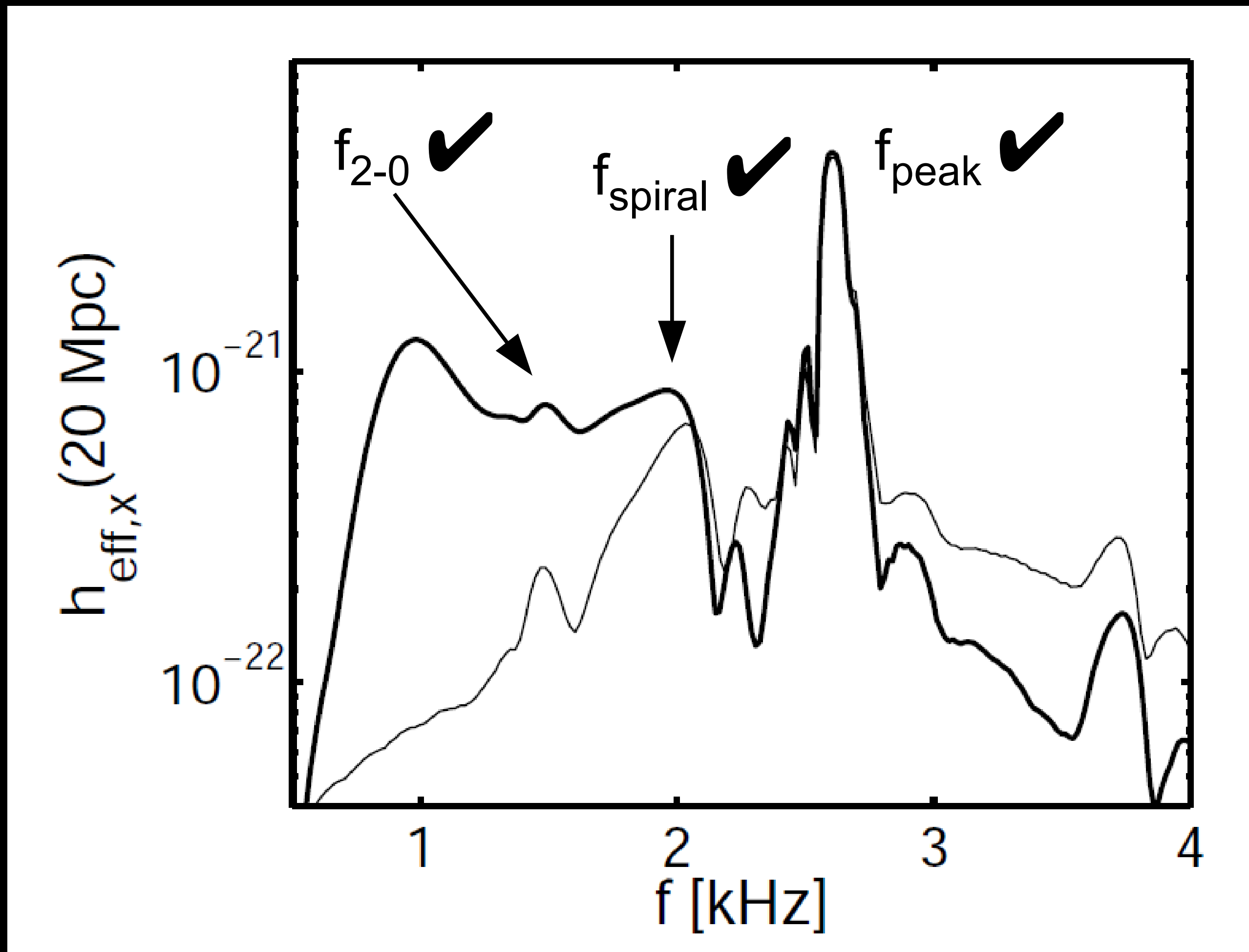

- Orbital motion of antipodal bulges generate peak at f_{spiral}

Further evidence

- Presence of spiral pattern coincides with presence of peak in GW spectrum (different time windows for FFT)
- Mass of bulges (several 0.1 M_{sun}) can explain strength of the peak by toy model of point particles the central remnant for a few ms
- Tracing dynamics / GW emission by computing spectra for "outer" and "inner" remnant → f_{spiral} emission "is produced outside"
- Dynamics of double cores (inner remnant) fail to explain this emission
- Spectrogram agrees with this picture (length, frequency), no strong time-variation of the dominant frequency

=> orbital motion => f_{spiral} peak

Example: TM1 1.35-1.35 Msun, strong tidal bulges, weak radial oscillation (e.g. from analysis of lapse)

Clark et al. 2016

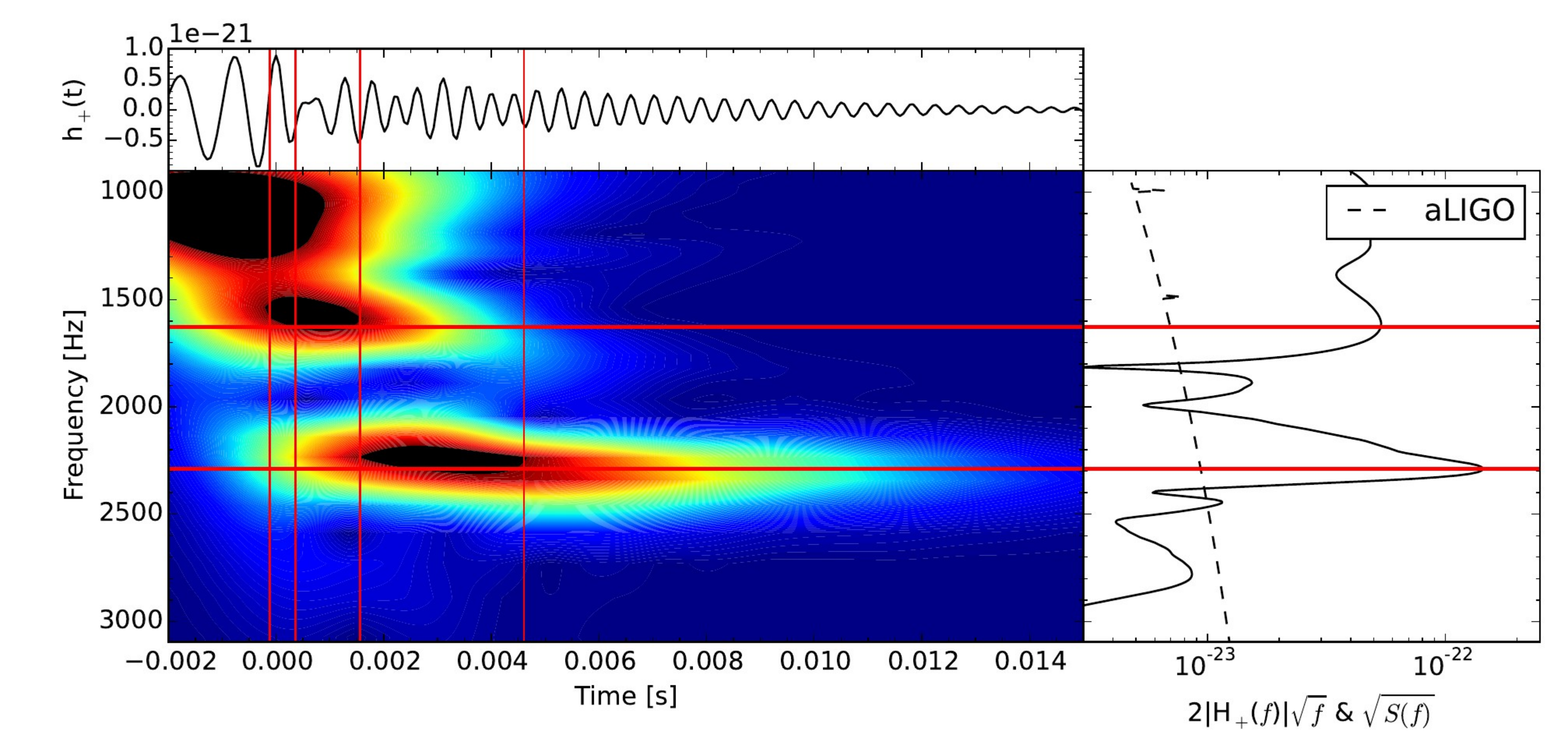

Note: different ideas about the origin of the peaks, e.g. Kastaun & Galeazzi 2015, Takami et al. 2014, 2015 propose a strongly varying instantaneous frequency that produces side peaks

SFHO 1.35-1.35 Msun, weak tidal bulges, strong radial oscillation

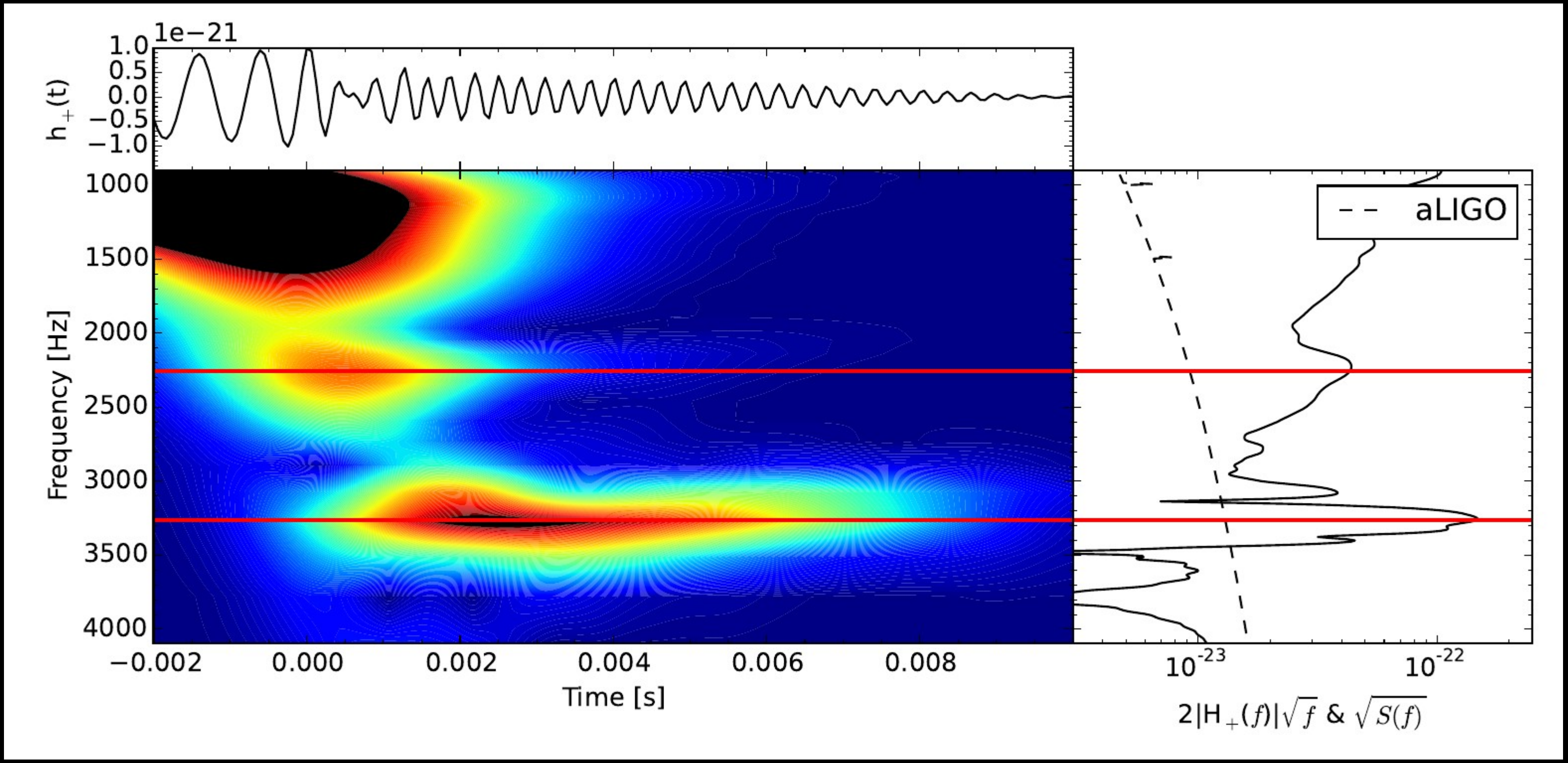

Clark et al. 2016

Discrete features !

Unified picture of postmerger GW emission and dynamics – a classification scheme

Survey of GW spectra

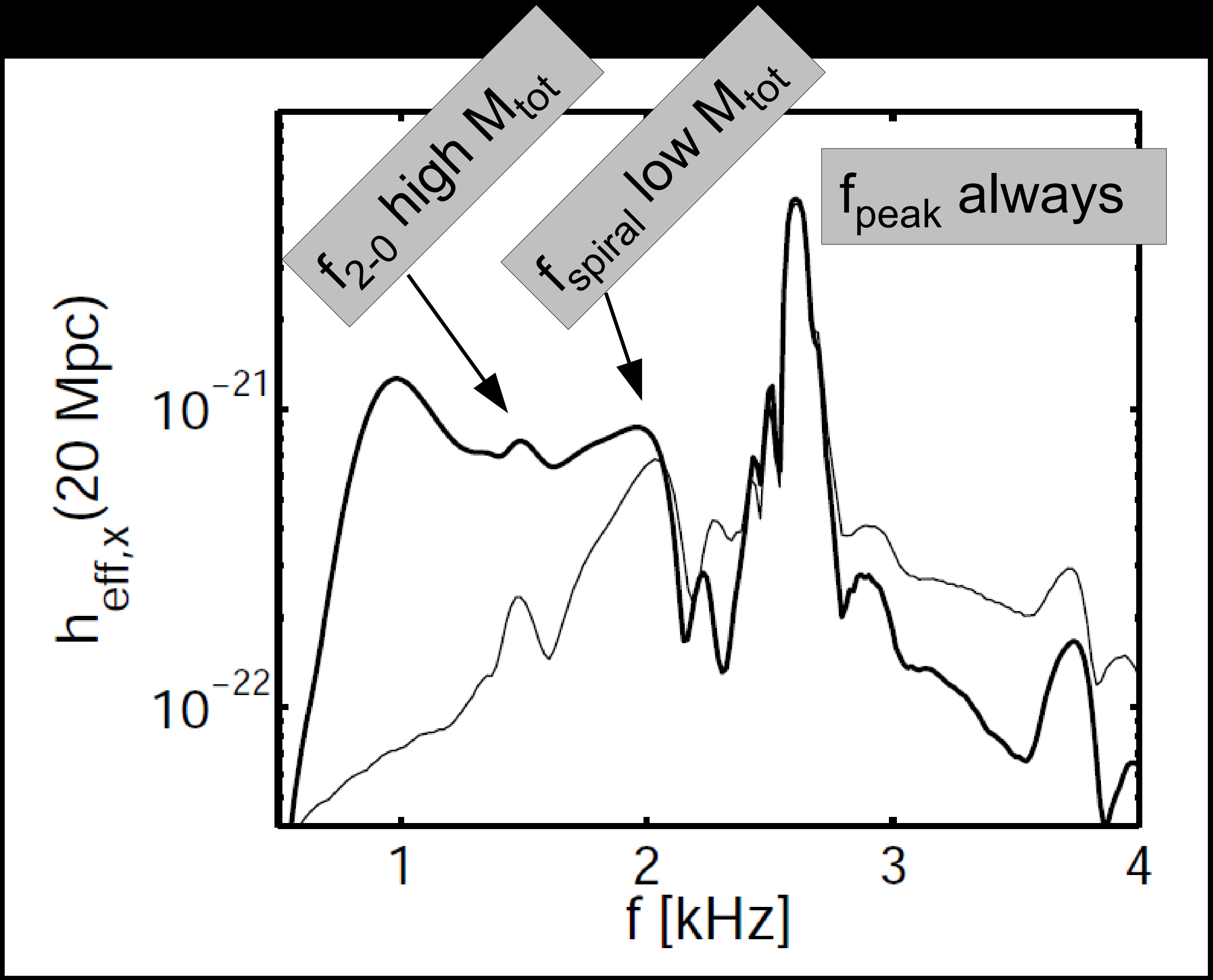

- Quantitative analysis of many models to identify which features is what
- Considering different models (EoS, M_{tot}): 3 types of spectra depending on presence of secondary features (dominant f_{peak} is always present)

Bauswein & Stergioulas 2015

Survey of GW spectra

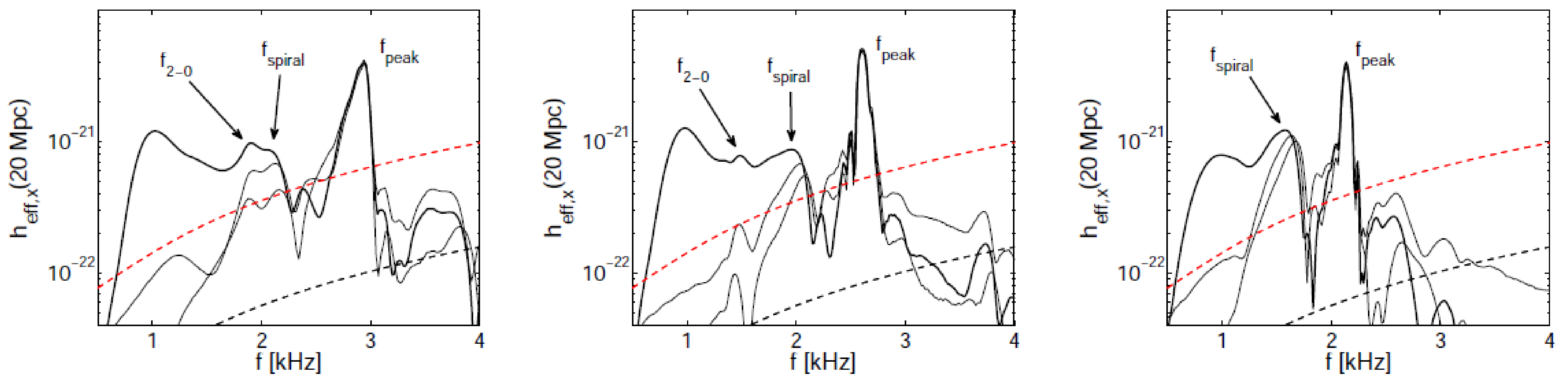

Type I Type II Type III

LS220, DD2, NL3 EoS all with M_{tot} = 2.7 M_{sun} → consider M_{tot} relative M_{thres}

=> Depending on binary model (EoS, M1/2) either one or the other or both features are present / dominant

=> you measure a secondary peak you should always think whether it is f_{2-0} or f_{spiral}

Classification scheme

- Type I: 2-0 feature dominates, f_{spiral} hardly visible, radial mode strongly excited, observed for soft EoS, relatively high M_{tot}
- Type II: both secondary features have comparable strength, clearly distinguishable, moderate binary masses
- Type III: f_{spiral} dominates, f_{2-0} hardly visible, found for stiff EoS, relatively low binary masses, (central lapse, GW amplitude, rhomax show low-frequency modulation in addition to radial oscillation)

- Different types show also different dynamical behavior, e.g. in central lapse, maximum density, GW amplitude, ….
- High mass / low mass relative to threshold binary mass for prompt BH collapse (→ EoS dependent)
- Continuous transition between different types: a given EoS shows all types depending on M_{tot}: Type III for low M_{tot} → Type I towards M_{thres}

Bauswein & Stergioulas 2015

Classification scheme

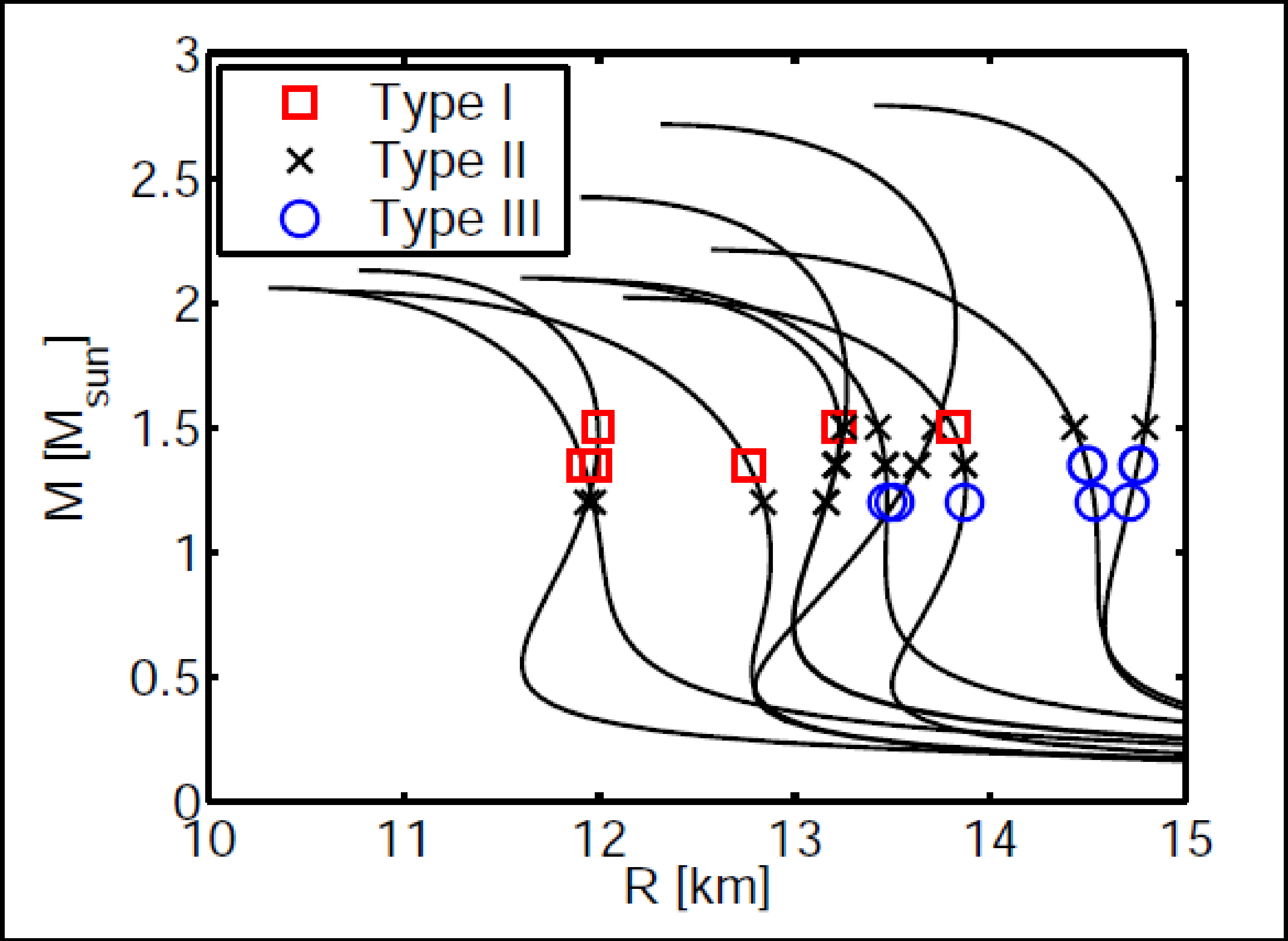

Type of M_1-M_2 merger indicate at $M_{tot}/2 = M_1$

Bauswein et al. 2015

(Continuous transition between types → tentative association)

For M_{tot} = 2.7 M_{sun} all Types are possible depending on EoS

Classification intuitive: merger dynamics affected by compactness

Classification scheme

- Behavior understandable:

- Type I: compact NSs merge → high impact velocity / violent collision => radial oscillation strongly excited (2-0 dominant); higher compactness → formation of tidal bulges suppressed (f_{spiral} weaker)

- Type III: less compact NSs merge → lower impact velocity / smooth merging => radial mode suppressed (no 2-0); pronounced tidal bulges (strong f_{spiral} feature)

- For Type III and Type II low-frequency modulation with $f_{low} = f_{peak} - f_{spiral}$ by orientation of bulge w. r. t. inner double-core/bar

- (seen in lapse, GW amp., rhomax, ...)

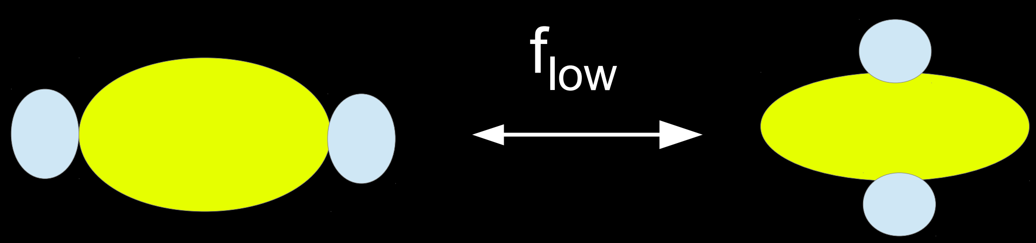

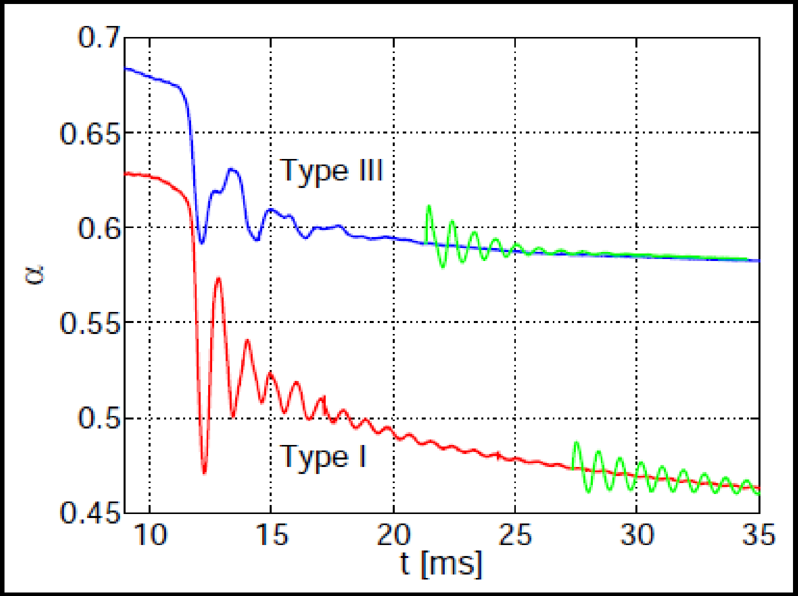

Dependencies of secondary features

Dependencies of secondary frequencies

EoS characterized by compactness C=M/R of inspiralling stars (equivalent to radius as before)

Bauswein et al. 2015

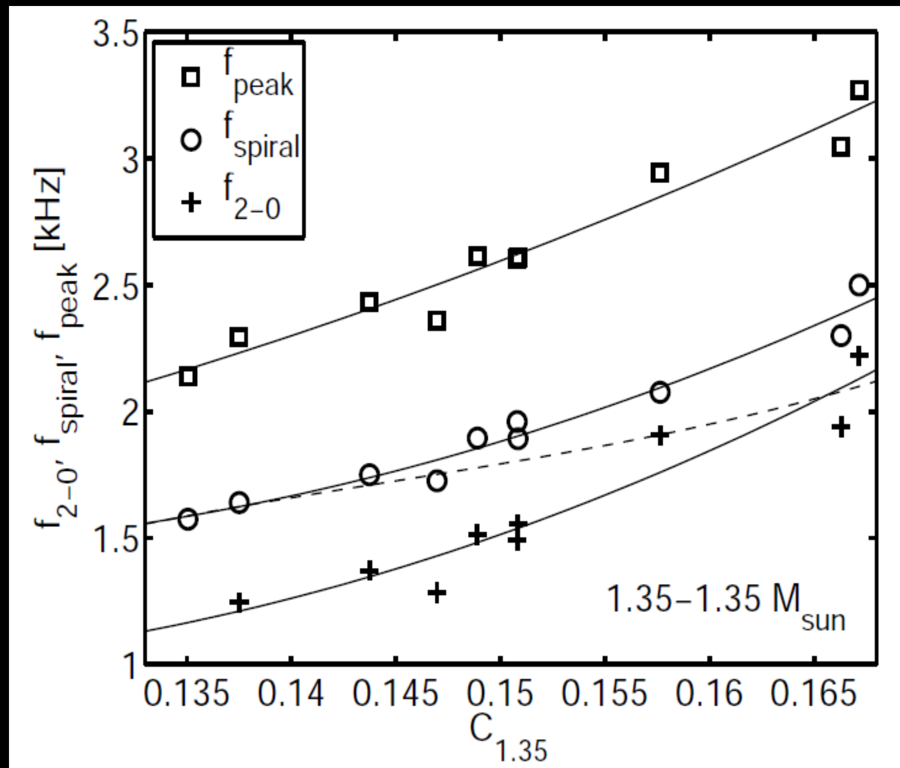

For fixed M_{tot} = 2.7 M_{sun}

Dashed line from Takami et al. 2014

- All three frequencies scale similarly with compactness (equivalently radius since M = $M_{tot}/2$ = fixed here)
- If subdominant peaks with comparable strength → risk of confusion / misinterpretation of measured frequency
- Here: only temperature-dependent EoS to avoid uncertainties/ambiguities due to approximate treatment of thermal effects (Gamma_th)
- For small binary mass asymmetry only small quantitative shifts
-

Different binary masses

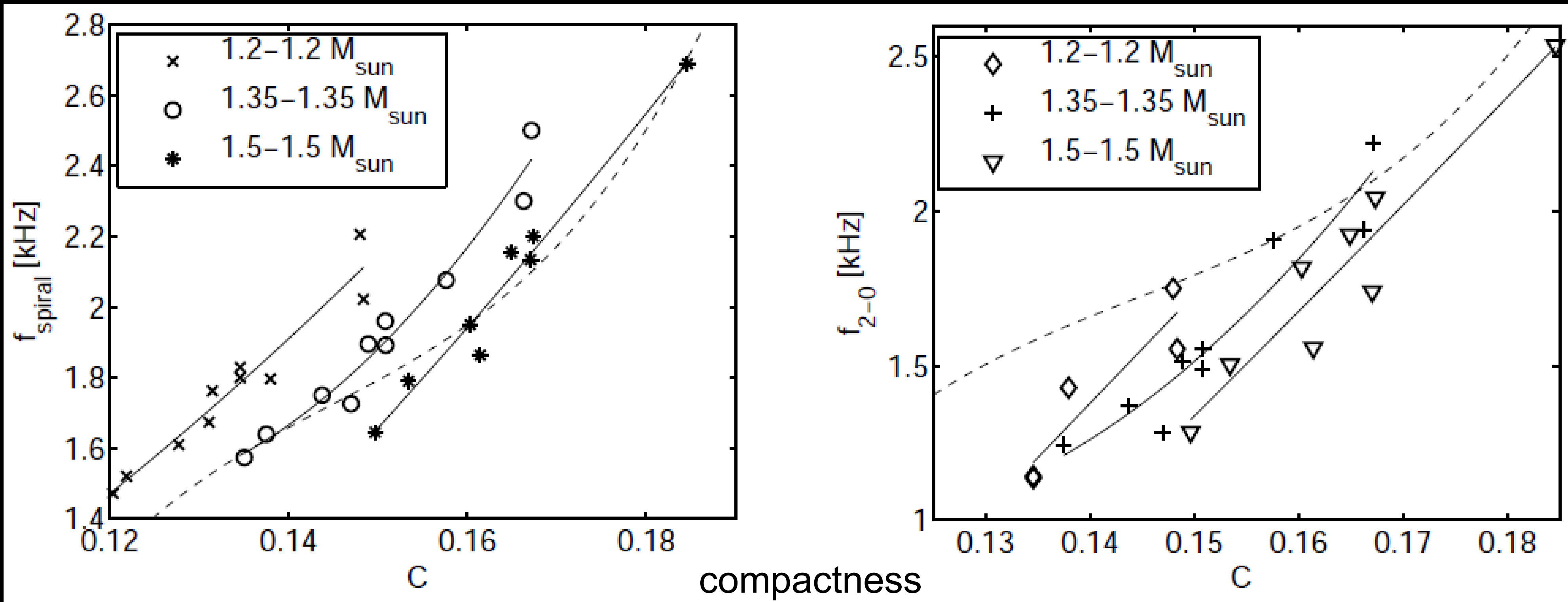

Bauswein et al. 2015

Dashed line from Takami et al. 2014

- for the individual secondary frequencies there are relations between C and the frequency for fixed binary masses (solid lines)
- (binary masses will be known from GW inspiral signal)
- no single, universal, mass-independent relation (for a expected range of binary masses), also when choosing the strongest secondary peak (risk of confusing subd. peaks)

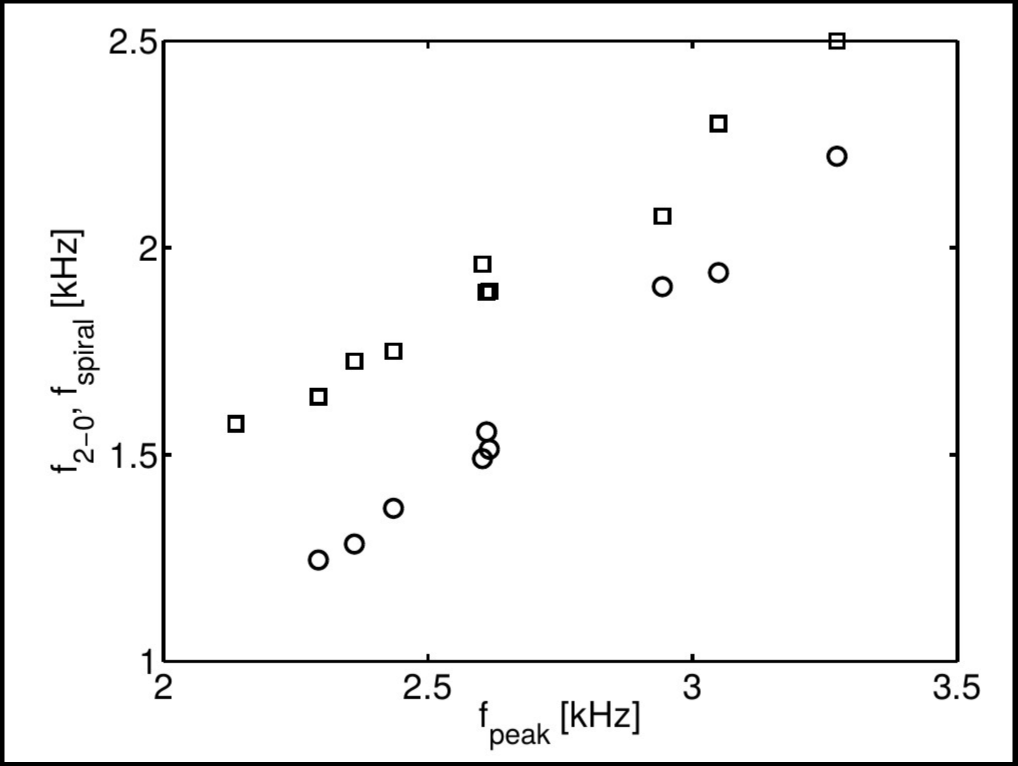

1.35-1.35 Msun

Clark et al. 2016

→ secondary frequencies are essentially given by dominant frequency

Universality of GW spectrum

Symmetric binaries

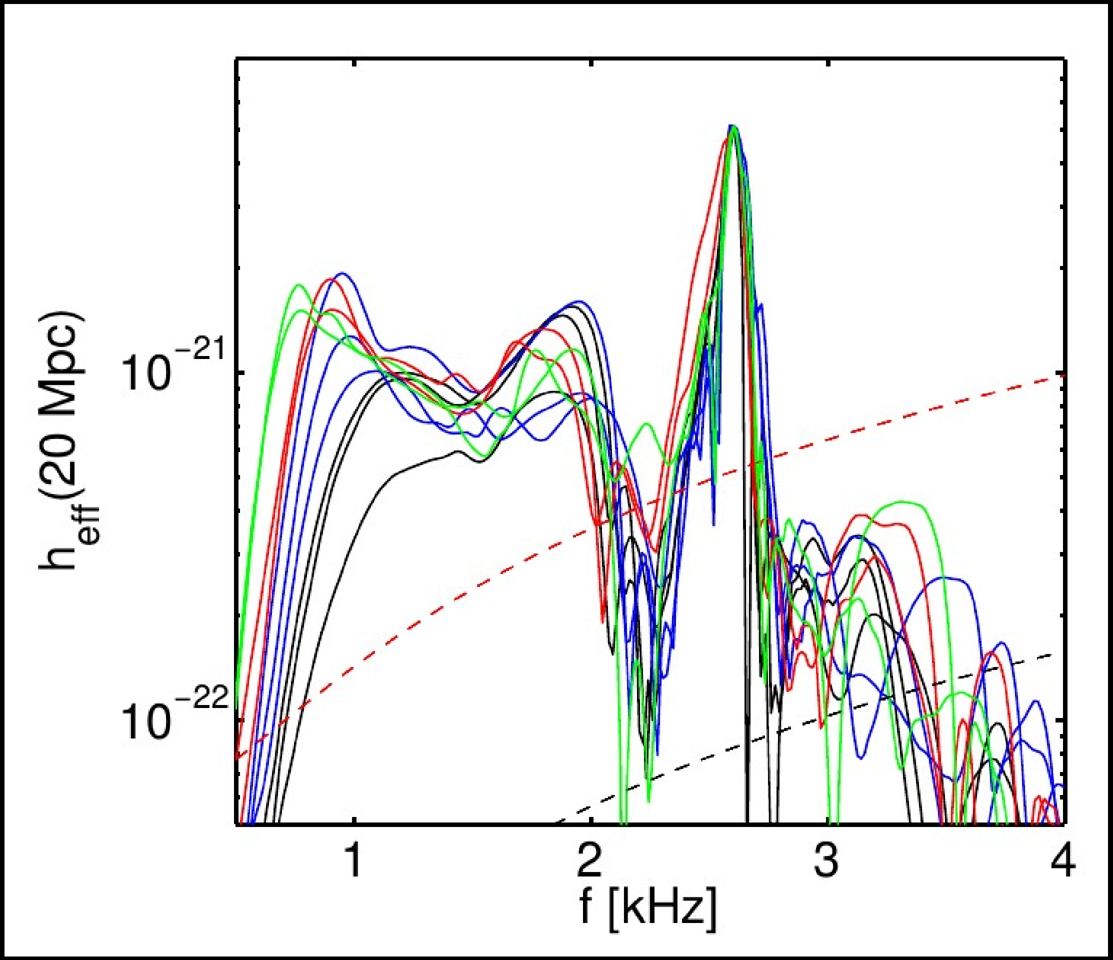

$af_{\rm sec} = f_{\rm ref} f_{\rm sec}/f_{\rm peak}$

Bauswein et al. 2015

Rescaled to reference frequency f_{ref}=2.6 kHz with $a = f_{ref}/f_{peak}$

$$\Rightarrow af_{sec} = f_{ref} f_{sec}/f_{peak} = f_{ref} \cdot const$$

→ universal spectrum basis of using PCA for GW data analysis

Analytical model of postmerger GW emission

$$
\begin{aligned}
h_\times \propto Q_{xy} = {} & A_{\mathrm{peak}} \exp\left(-(t-t_0)/\tau_{\mathrm{peak}}\right) \\
& \sin\left(2\pi f_{\mathrm{peak}}(t-t_0) + \phi_{\mathrm{peak}}\right) \\
& + A_{\mathrm{spiral}} \exp\left(-(t-t_0)/\tau_{\mathrm{spiral}}\right) \\
& \sin\left(2\pi f_{\mathrm{spiral}}(t-t_0) + \phi_{\mathrm{spiral}}\right) \\
& + A_{2-0} \exp\left(-(t-t_0)/\tau_{2-0}\right) \\
& \sin(2\pi f_{2-0}(t-t_0) + \phi_{2-0}),
\end{aligned}
$$

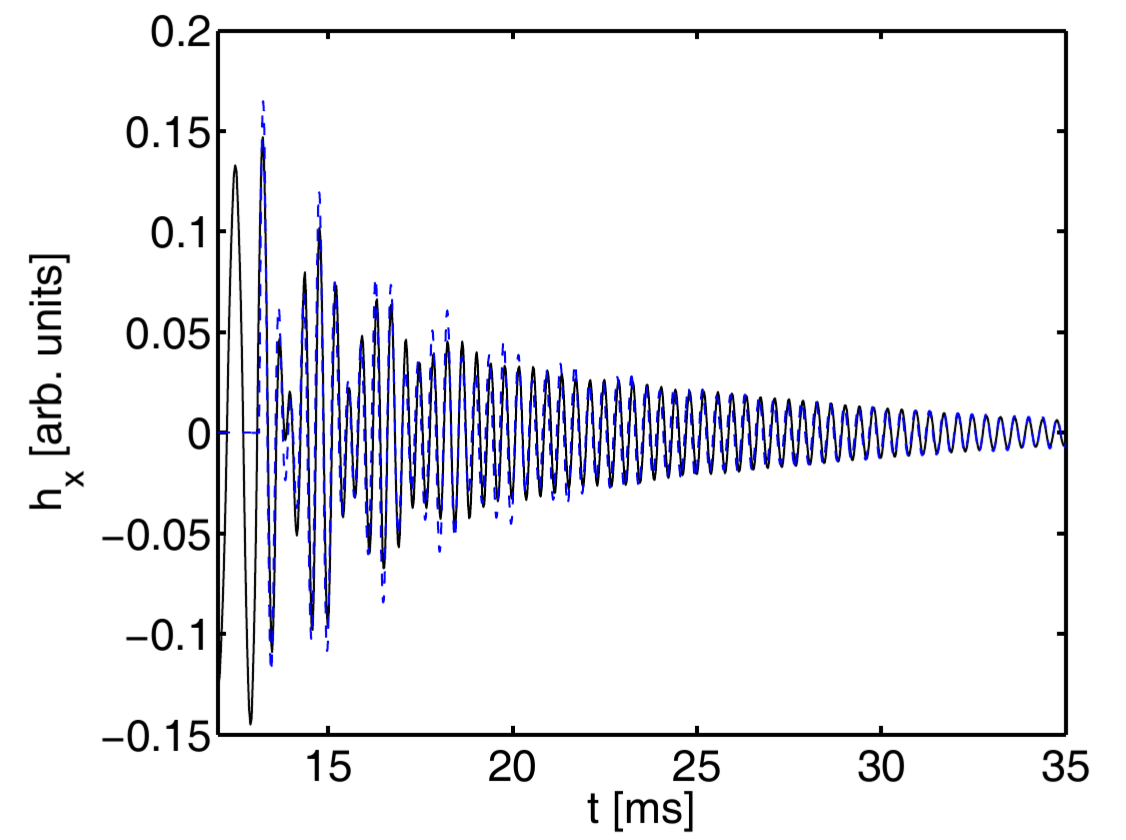

Parameter tuning only by eye !

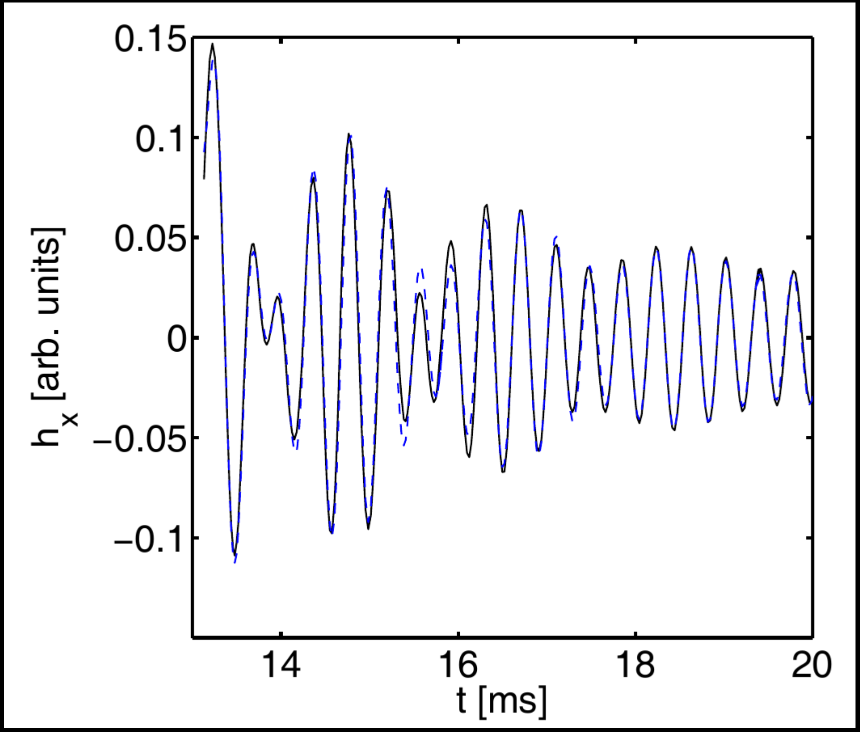

fit

Bauswein et al. 2016

Conclusions

- NS radius measurable from dominant postmerger frequency
- Explicitly shown by GW data analysis
- Threshold binary mass for prompt collapse → maximum mass M_{max}
- Semi-analytic model reproduces collapse behavior
- Mass dependence of f_{peak} → M_{max} and R_{max}

  → constrain high-density EoS
- Different mechanisms generate subdominant GW peaks
- Classification scheme of postmerger GW spectra based on presence/strength of secondary peaks (physically motivated)

Details: